Astron. Astrophys. 261, 164–187 (1992)

ASTRONOMY AND ASTROPHYSICS

Fluorine in red giant stars: evidence for nucleosynthesis

A. Jorissen*, V.V. Smith, and D.L. Lambert****

Department of Astronomy, University of Texas, Austin, TX 78712, USA

Received September 13, 1991; accepted January 12, 1992

Abstract. Fluorine abundances for red giants of type K, Ba, M, MS, S, SC, N, and J were obtained from the rotation–vibration lines of the molecule HF. There appears to be a clear correlation between [F/O] and $^{12}C/^{16}O$ since N stars display F abundances up to 30 times the solar system value. This correlation points toward the He-burning shell as the site of F synthesis. The nuclear chain $^{14}N(\alpha,\gamma)^{18}F(\beta^+)^{18}O(p,\alpha)^{15}N(\alpha,\gamma)^{19}F$ (where protons come from $^{13}C(\alpha,n)^{16}O$ followed by $^{14}N(n,p)^{14}C$) operating at the very beginning of He-burning is the most likely for ^{19}F production in thermal pulses. The initial ^{13}C supply then acts as a limiting factor for the ^{19}F yield. It is shown that the secondary ^{13}C supply from the CNO cycle ashes can account for the F abundances of most of the S and N stars, although the most F-enriched stars may require a primary ^{13}C supply. This is well in line with the fact that the most F-rich S stars also show a CNO excess ($[\Sigma CNO/Fe] \gtrsim 0.1$) due to enhanced N. Other nuclear paths are investigated, but none of them appears to be efficient enough.

Our ^{19}F abundances can in principle be used to probe the temperature of the thermal pulse, since $^{19}F(\alpha,p)^{22}Ne$ did not destroy ^{19}F. However, the method is quite sensitive to the fine structure of thermal pulses, namely to the dredge-up depth, to the retreat rate of the convective shell after its maximum extension and to the time evolution of temperature in the pulse. The $^{19}F(\alpha,p)^{22}Ne$ rate itself is still uncertain.

Since the current rate for $^{19}F(\alpha,p)^{22}Ne$ is at least 20 times faster than $^{22}Ne(\alpha,n)^{25}Mg$ in the $2.0 \lesssim T_8 \lesssim 3.5$ temperature range, ^{19}F cannot survive in layers where neutrons are being liberated by $^{22}Ne(\alpha,n)^{25}Mg$. This may constitute a further argument against the operation of that neutron source in asymptotic giant branch stars.

Our observations also point toward asymptotic giant branch stars as being major contributors to the galactic F production. The F content of the metal-deficient star α Boo ($[Fe/H] = -0.6$, $[F/Fe] = 0$, $[F/O] = -0.5$) also weakens the claim by Woosley et al. (1990) that SN II are instead responsible for the galactic F production, since F should then follow O rather than Fe.

Finally, F is found to be overabundant in barium stars, although it is solar in normal K giants. This provides a further support to the mass transfer hypothesis as the origin of the barium star peculiarities, since the dilution factor of the accreted material in the envelope of barium stars deduced from C, F, and heavy elements are consistent with each other.

Key words: stars: abundances – nucleosynthesis

1. Introduction

Fluorine is one of the few chemical elements (its only stable isotope being ^{19}F) whose nucleosynthetic origin is still much debated. This is due to both the fragility of the nuclide, which is readily destroyed by proton or α captures in stellar interiors, and to the difficulty of observing F in stellar spectra because of the lack of useful lines in the visual region of the spectrum. The solar system has long been the only source of information about the F abundance in the Galaxy. Anders & Grevesse (1989) give a meteoritic value of 4.48 ± 0.06 (on the $\log N_H = 12.0$ scale) and quote a solar photospheric abundance (from observations of the HF molecule in sunspots) of 4.56 ± 0.30 and a solar coronal value of 4.00 ± 0.30. In the solar system, fluorine is thus by far the least abundant of all the $12 \leq A \leq 32$ nuclides (A being the mass number).

Theories of stellar nucleosynthesis have not yet been able to identify clearly the origin of the solar system's fluorine. Various astrophysical sites for F production have been suggested. In the context of explosive H-burning in novae, Woosley (1986) found a substantial F production when crudely approximating the effects of mass loss and convective mixing by a two-zone model. Goriely et al. (1989) emphasized the merits of He-burning, either during shell burning in massive stars, during thermal pulses in low- or intermediate-mass stars, or in more exotic situations leading to the mixing of protons in a He-burning zone, giving rise to the $^{13}C(\alpha,n)^{16}O$ neutron source. Finally, Woosley & Haxton (1988) and Woosley et al. (1990) invoked a "ν-process": just above the collapsing core of a Type II supernova, in the layer enriched in ^{20}Ne by the previous C-burning phase, the stupendous flux of neutrinos can excite ^{20}Ne to unbound levels by inelastic scattering, and the resulting evaporation of one proton from an excited ^{20}Ne nucleus can result in ^{19}F production.

In the present paper we describe our abundance determinations of F in several K giants and asymptotic giant branch (AGB) stars, using the infrared vibration–rotation lines of HF. These new data constitute the only available information about the

Send offprint requests to: A. Jorissen

* Present address: European Southern Observatory, K. Schwarzschild Str. 2, D/W-8046 Garching bei München, Germany

** Visiting Astronomer, Kitt Peak National Observatory, National Optical Astronomy Observatories, which is operated by the Association of Universities for Research Inc., under contract with the National Science Foundation.

fluorine abundance outside the solar system and provide invaluable clues to the question of the nucleosynthetic origin of F. Previous observations of extra-solar F are limited to very uncertain abundance determinations from a [F IV] emission line in high excitation planetary nebulae (Aller 1978; Aller & Czyzak 1983). Stellar HF lines were identified first in α Ori by Spinrad et al. (1971) and a tentative identification of circumstellar AlF lines in IRC+10216 by Cernicharo & Guélin (1987) was reported. Our observations not only confirm that F production occurs at a He-burning site, but are also able to constrain the current models of AGB stars.

Three different kinds of events may result in nucleosynthesis during AGB evolution (see Iben & Renzini 1983 for a review). The first event is related to the recurrent thermal instability ("thermal pulse") affecting the He-burning shell of AGB stars. When the He-burning shell is thin and close enough to the overlying H-burning shell, thermal runaways of the energy production by the He-burning shell occur, and the He-burning convective shell extends to encompass the former intershell zone. As a result, ashes of the H-burning shell and of the previous thermal pulse are mixed within the convective zone where He-burning occurs. Iben (1975) initially suggested that heavy element synthesis occurs via the s-process in the convective shell through the neutrons released by $^{14}N(\alpha,\gamma)^{18}F(\beta^+)^{18}O(\alpha,\gamma)^{22}Ne(\alpha,n)^{25}Mg$, with ^{14}N abundantly present in the H-burning ashes. But this suggestion is still a matter of controversy (see Lattanzio 1989; Arnould 1991, for recent reviews), as are the conditions necessary for the occurrence of the third dredge-up. This event corresponds to the inwards extension of the outer convective envelope in regions previously processed by the thermal pulse, thus bringing to the surface the fresh nuclear products.

Heavy element synthesis has also been predicted to occur in the (rare?) situations where the He-burning convective shell can make contact with the overlying H zone (combined H- and He-burning, or HHe-b), since neutrons can then be released through $^{12}C(p,\gamma)^{13}N(\beta^+)^{13}C(\alpha,n)^{16}O$. Iben (1976) and Fujimoto (1977) have shown that the contact between the two zones is generally prevented by the large difference in the entropy content of the considered regions. Particular situations where contact can be established are large luminosity thermal pulses in stars with a low mass outer envelope (Schönberner 1979; Iben et al. 1983). A slightly different way of achieving HHe-b has been found by Sackmann (1980), Iben & Renzini (1982a, b), and Hollowell & Iben (1989, 1990) and involves "semiconvective" mixing of protons from the H zone into the C pocket produced by the thermal pulse, shortly after the retreat of the convective shell from the intershell zone. Neutrons are produced in the next thermal pulse when the ^{13}C resulting from the semi-convective mixing is engulfed in the convective He shell.

Finally, the third kind of nucleosynthesis event associated with AGB stars involves the suggestion that the temperature at the base of the outer convective envelope can be high enough to trigger proton captures by several nuclei, resulting in a progressive nuclear processing of the matter in the whole convective envelope (Scalo & Ulrich 1973; Sackmann et al. 1974; Despain & Scalo 1977; Renzini & Voli 1981). This process has sometimes been associated with ^7Li production (Scalo et al. 1975) and ^{26}Al production (Nørgaard 1980; Frantsman 1989).

After deriving the F abundances in Sect. 2, Sect. 3 will investigate the relevance of these AGB nucleosynthesis sites for ^{19}F production. Several possible nuclear paths will be considered, and their merits evaluated from general arguments, independently of the detailed structure of a particular stellar model. Detailed pulse computations, including a self-consistent treatment of the associated nucleosynthesis, can be found in a companion paper (Forestini et al. 1991; Paper I). Section 4 briefly addresses the question of the galactic origin of ^{19}F.

2. Observations and reductions

Our data consist of high-resolution infrared spectra near a wavelength of 2.2 μm obtained with the Kitt Peak National Observatory's 4 m telescope and Fourier Transform Spectrometer (FTS, Hall et al. 1978). These spectra were used for the CNO abundance analysis by Smith & Lambert (1990) in the case of the M, MS, and S stars, by Dominy et al. (1986) in the case of the SC stars, and by Lambert et al. (1986) for the N and J carbon stars. A few supplementary spectra of cool barium stars and normal K giants were also obtained from the FTS data archives. Typical apodized resolutions of these spectra ranged from 0.03 to 0.10 cm^{-1} ($R=\sigma/\Delta\sigma\approx 45\,000$–$160\,000$), and all program stars were ratioed with hot stars to remove, as well as possible, telluric spectral features.

In Table 1 we list the stars. The M, MS, and S stars are presented as one sample in Table 1 because the detailed heavy-element abundance analysis of Smith & Lambert (1990) does not always confirm the spectral type assigned from low-dispersion spectra: some stars classified as MS or S in Stephenson's (1984) catalogue were found to have normal heavy-element abundances ("Stephenson M stars"), while three M giants (HR 4647, HR 5299, and HR 6146) are slightly s-process enriched.

Table 1. The various samples of red giants analyzed

Normal K giants		
γ Dra		K5 III
β UMi		K4 III
α Ser		K2 III
α Boo		K2 IIIp
Cool barium stars		
HD 121447		
HD 178717		
M, MS, and S stars		
HR 337	β And	M0 III[f]
HR 1105	BD Cam	S5, 3[b]
HR 1556	o^1 Ori	M3 III S[g]
BD +48°1187	TV Aur	S5/6[-a]
HD 35155		S3/2[a]
BD +14°1350	DY Gem	S8, 5[b]
HD 49368		S3/2[a]
HD 58521	Y Lyn	M6S[b]
HD 64332	NQ Pup	S4.5/2[-a]
BD +06°2063		M3S[c,i]
HR 3639	RS Cnc	M6 IIIa S[g]
HD 96360		M3Swk[d,i]
HR 4483	ω Vir	M4+IIIab[g]
HR 4647		M4 III[f]
BD−02°3726		M1Swk[d]
HR 5226	10 Dra	M3 IIIaS[g]
HR 5299		M4+III[g,j]

Table 1 (continued)

BD + 57° 1671		M2S[d]
HR 6146	30 Her	M6 III[f,j]
BD −13° 4495		M2S[d,i]
BD −18° 4320		Swk[d]
HR 6702	OP Her	M5 + II[h]
BD +16° 3426		M4Swk[d,i]
HD 172804	V679 Oph	S5/6[−a]
HD 189581		S4*2[e,i]
HD 199799		MS[d]
HR 8062		M4 IIIaS[g]
HR 8775	β Peg	M2 + III[g]
SC Stars		
HD 44544	FU Mon	S6.5/7.5[a,k]
HD 198164	CY Cyg	SC2/7.5[a]
HD 209890	RZ Peg	SC5−9/9−e[a]
HDE 286340	GP Ori	SC7/8[−a,k]
N and J stars[l]		
AQ Sgr		N3
BL Ori		N0
R Lep		N6; C7,4+
R Scl		Np; C6,5; J
RT Cap		N
RV Cyg		N5; C6,4
RY Dra		N4; C4, 4; J
S Sct		N3; C5,4
ST Cam		N5; C6,4
T Lyr		Np; C6,5; R6; J
TU Gem		N3; C4,6
TW Oph		Nb; C6,5
TX Psc		N0; C6,2
U Cam		N5; C6, 4e
UU Aur		N3; C5,3
UX Dra		N0; C7,3
V460 Cyg		N1; C6,3; R
V Hya		N; C7,5
VY UMa		N0; C6,3; R8
W CMa		N; R8
W Ori		N5; C5,3
WZ Cas		N1p; C9,1; J
X Cnc		N3; C5,4
Y Hya		N3; C5,4
Y CVn		N3; C5,4; R
Y Tau		N2; C7,4e
Z Psc		N0; C7,3

[a] Keenan & Boeshaar (1980); [b] Keenan (1954); [c] Ake (1979); [d] Stephenson (1984); [e] MacConnell (1982); [f] Hoffleit (1982); [g] Yamashita (1967); [h] Classified as M6S by Jaschek et al. (1964). Yamashita (1967) notes YO-enhanced; [i] "Stephenson M star"; [j] Smith & Lambert (1990) found slightly enhanced s-process elements; [k] Also classified as J by Yamashita (1972); [l] From Lambert et al. (1986)

Vibration–rotation lines of the 1–0 band of HF were identified in our sample of red giants using the laboratory frequencies of Webb & Rao (1968) or predicted frequencies from Tipping (1989): in the M giants all lines from R8 to R21 were identified within our spectral window. Rotational lines below R8 ($\sigma = 4256.31\ cm^{-1}$) were at frequencies near the low-frequency end of the K-band filter where telluric contamination becomes severe, while higher-lying lines above R21 became very weak. In these cool giants, blending with CO and CN lines can be a problem and, for our abundance analysis, all HF lines were checked for blends. It was found that the best lines for an abundance analysis were the R9, R13, R14, R15, and R16 lines. Even in this "cleaned" list, the R9 line becomes obliterated by a nearby $^{12}C^{16}O$ line in the cooler (M, MS, S, and C stars) red giants, while the R13 and R14 lines are blended by weak CN lines which must be included in a spectrum synthesis (for the R13 line the offending CN lines are the 2–4 R_1 63 and 0–2 Q_2 68 lines of ^{12}CN, while for R14 it is 0–2 Q_2 73 of ^{13}CN). In Table 2 we present the HF lines used in the abundance analysis with frequency, excitation potential, and gf value. The accurate oscillator strengths were calculated using the Einstein A-values kindly provided by Tipping (1989).

Table 2. HF lines used in the abundance analysis

Line		$\sigma\ (cm^{-1})$	ξ'' (eV)	gf
(1–0)	R9	4279.95	0.48	$1.11\,10^{-4}$
	R13[a]	4354.59	0.71	$1.15\,10^{-4}$
	R14[a]	4368.14	0.78	$1.14\,10^{-4}$
	R15	4379.60	0.85	$1.12\,10^{-4}$
	R16	4388.94	0.93	$1.09\,10^{-4}$

[a] These lines are contaminated by weak CN lines which are included in the fluorine abundance analysis.

Figure 1 presents sample spectra for a K giant (γ Dra), a barium star (HD 121447), an M giant (β Peg), and an S star (DY Gem) showing the HF (1–0) R16 line. Figure 2 shows the R13, R14, R15, and R16 lines in the MS star HD 199799.

The method of analysis, described by Smith & Lambert (1985, 1986, 1990), involves the comparison of observed equivalent widths with predicted LTE equivalent widths computed from model atmospheres using a modified form of the spectrum synthesis code from Sneden (1974). The model atmospheres are from Bell et al. (1976) for the K giants, from Johnson et al. (1980) for the cool barium, M, MS, and S stars, from Johnson (1982) for the SC stars, and from Lambert et al. (1986) for the N and J carbon stars.

We adopted the stellar parameters (T_{eff}, $\log g$, and microturbulence ξ) derived by the previous studies: Smith (1984) for the cool barium stars, Smith & Lambert (1990) for the M, MS, and S stars, Dominy et al. (1986) for the SC stars, and Lambert et al. (1986) for the N and J stars. These parameters are assembled in Table 3, along with the HF equivalent widths. As mentioned before, the R13 and R14 lines can suffer significant CN contamination, and these lines were synthesized with the CN lines included and the resultant spectral feature was integrated for its total equivalent width.

In the case of S stars, model atmospheres corresponding to a (solar) C/O ratio of 0.6 were used, although the actual value may be different. The impact of this inconsistency on the derived F abundance is not expected to exceed 0.2 dex, and an illustration of the effect of the C/O ratio is presented in Fig. 3, where the R16 line equivalent widths for our stars are plotted as a function of

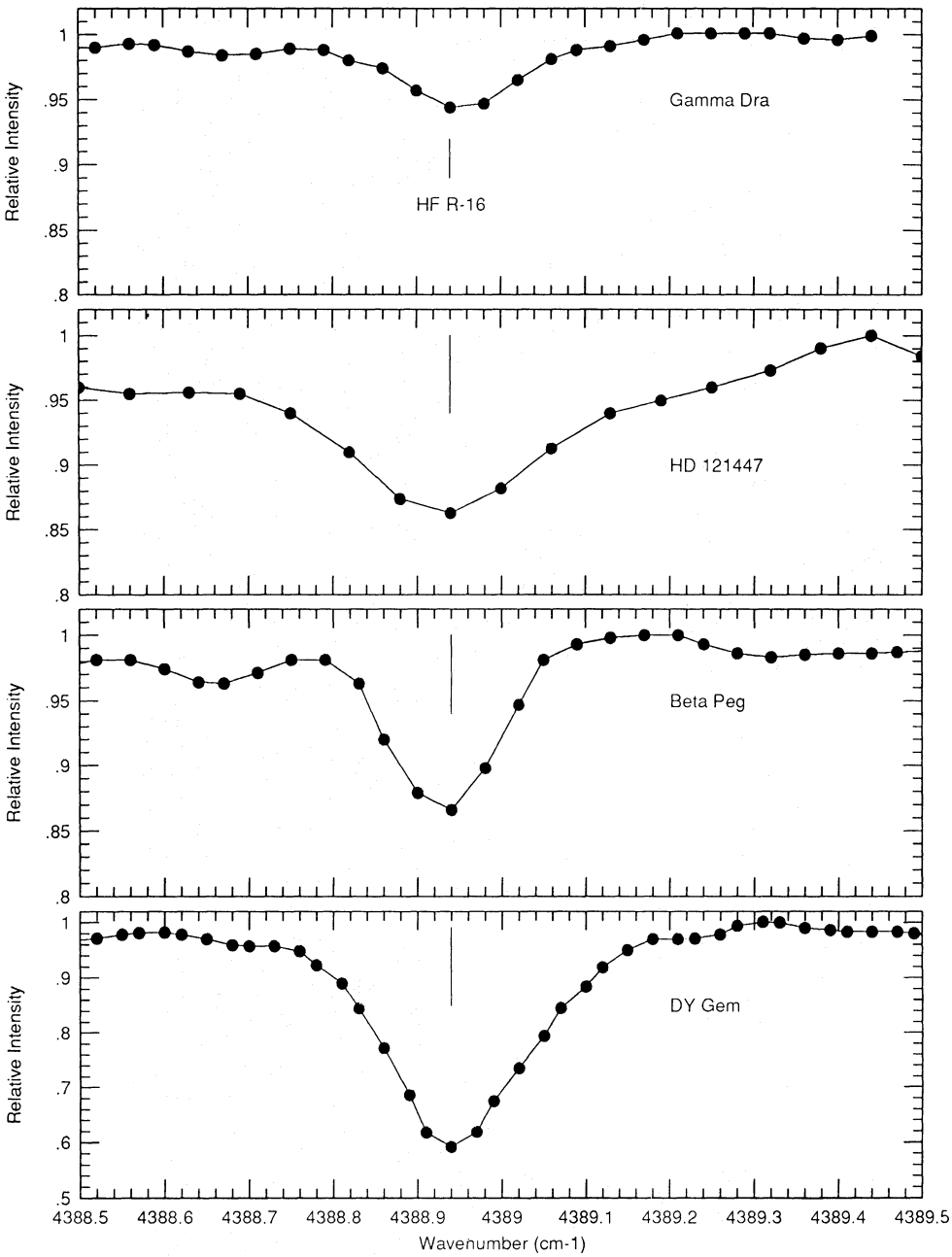

Fig. 1. Sample spectra of the HF R16 line in various types of red giants: a K giant (γ Dra), a barium star (HD 121447), an M giant (β Peg), and an S star (DY Gem) are shown

$T_{\rm eff}$, along with iso-abundance lines predicted from C/O = 0.6 model atmospheres ($T_{\rm eff} > 3000$ K) and from C/O = 1.1 model atmospheres ($T_{\rm eff} < 3200$ K). In the region of overlap, the abundances provided by the two sets of models differ by 0.2–0.3 dex, which is thus a good estimate of the uncertainty introduced by using models of inappropriate C/O values.

Fluorine abundances are presented in Table 4, on the scale where $\log\varepsilon(\mathrm{H}) = 12.0$, as well as normalized with respect to oxygen: $[\mathrm{F/O}] = (\log\varepsilon(\mathrm{F}) - 4.69) - [\log\varepsilon(\mathrm{O}) - \log\varepsilon_{\odot}(\mathrm{O})]$. Oxygen abundances were taken from Lambert & Ries (1981), Lambert et al. (1986), Smith & Lambert (1990), and the solar system abundance is taken from Anders & Grevesse (1989). The choice of the fluorine normalization will be described in Sect. 3.1. Also in Table 4, we include the overall metallicity of the star, [M/H], the total CNO abundances (ΣCNO) normalized to the stellar metallicity, and the $^{12}C/^{13}C$ ratios: all of these quantities were taken from the sources listed in the footnotes of Table 4. With the exception of WZ Cas, none of the stars in Table 4 is particularly "Li-rich", so we do not include the Li abundance, although Denn et al. (1991) list Li abundances for all of the carbon stars in Table 4. Figure 4 is a plot of $\log\varepsilon(^{19}\mathrm{F})$ versus $T_{\rm eff}$.

3. Analysis of the data

3.1. The ([F/O], $^{12}C/^{16}O$) correlation

Table 4 reveals that F is enhanced in all C and most S stars with respect to K and M giants. That result is illustrated in Fig. 5, displaying $\log\varepsilon(\mathrm{F})$ versus $\log\varepsilon(\mathrm{C})$, where the carbon abundances

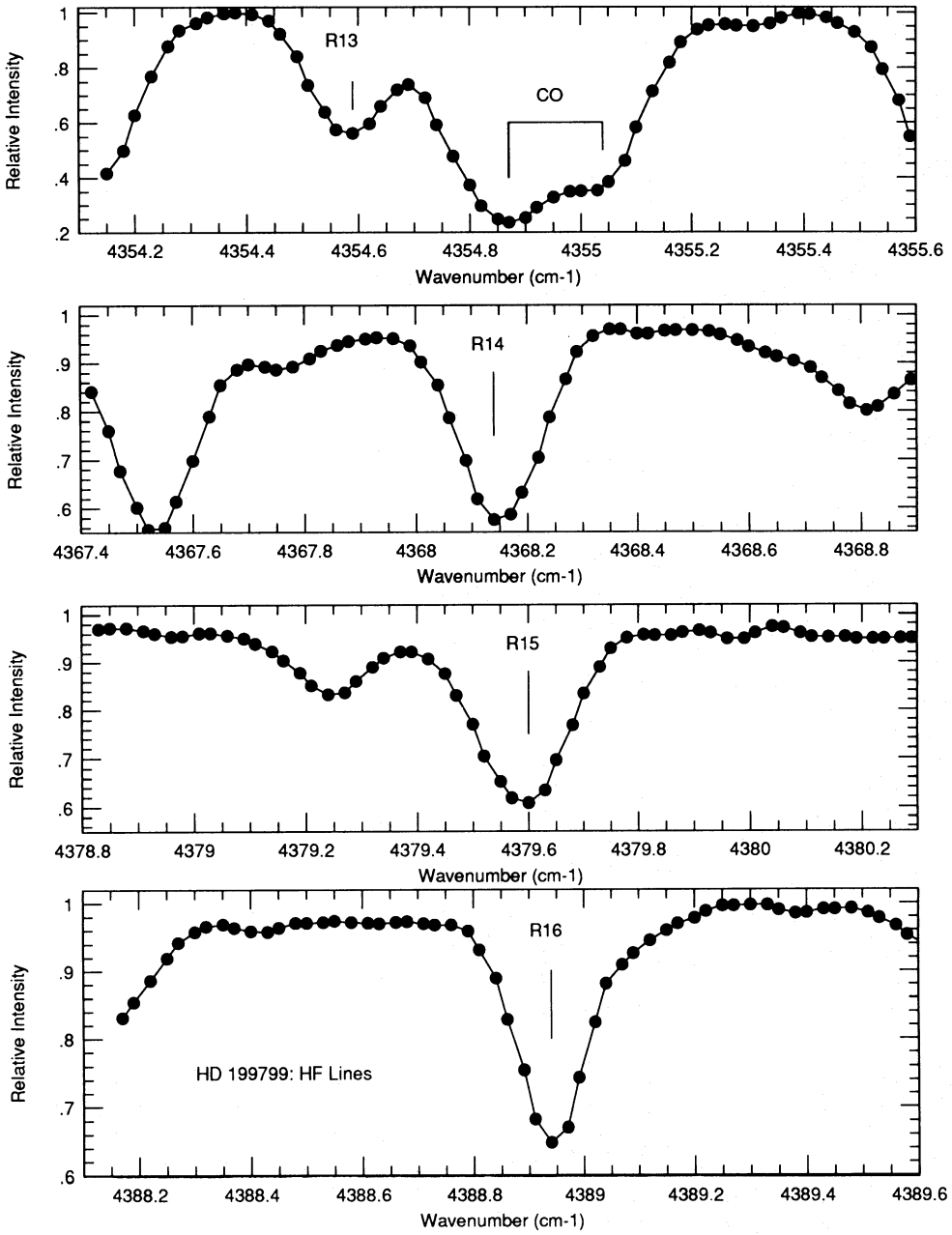

Fig. 2. The HF R13, R14, R15, and R16 lines are shown for the MS star HD 199799

are taken from Lambert & Ries (1981), Lambert et al. (1986), and Smith & Lambert (1990). Two different effects control the position of a star in that diagram, namely the alteration of the surface F and C abundances during the stellar lifetime (resulting from internal nucleosynthesis processes followed by envelope mixing, or from mass transfer across a binary system) and the stars' differing primordial compositions. The latter effect is especially apparent from the outstanding location of the metal-poor giant α Boo ($[Fe/H] = -0.56$). A very clear lower boundary to the region populated by stars in the ($\log \varepsilon_F$, $\log \varepsilon_C$) plane might reflect the effects of galactic chemical evolution, but that boundary is also affected by the first (and possibly second) dredge-up(s). As a result of the first dredge-up, it is well known that the surface C abundance of red giants is reduced by ~ 0.25 dex (see Smith 1990 for a review), the exact value being slightly dependent upon the stellar mass as predicted by theoretical models.

Up to now, only one theoretical study devoted to the first dredge-up provides some information about ^{19}F. Figure 3 of Landré et al. (1990) presents the variation of the ^{19}F abundance as a function of depth in a $15M_\odot$ star at the end of its main sequence lifetime. From that figure, one may infer that the first dredge-up will have no measurable effect on the surface ^{19}F abundance in this $15M_\odot$ star. Although this result for a massive star is not directly relevant in the context studied here, Landré et al. (1991) note that the trends observed in their $15M_\odot$ model are similar for less massive stars. Simple arguments based on the involved nuclear reaction rates can be used to confirm that F is unaffected by the first dredge-up. For the relevant temperature range ($1\,10^7 \lesssim T \lesssim 2\,10^7$ K), $^{18}O(p,\alpha)^{15}N$ is 100–1000 times faster than $^{18}O(p,\gamma)^{19}F$, according to Caughlan & Fowler (1988; hereafter CF88). In other words, one out of 100–1000 ^{18}O nuclei is converted into ^{19}F instead of ^{15}N. But since $^{19}F/^{18}O \sim 1/60$ in

Table 3. Model atmosphere parameters and HF equivalent widths

Star	$T_{\rm eff}$ (K)	log g	ξ (km s^{-1})	HF (1–0) equivalent widths in cm^{-1} 10^{-3}				
				R9	R13	R14	R15	R16
γ Dra	3980	1.9	2.0	29	20	17	12	7
β UMi	4340	1.9	2.0	16	9	—	—	—
α Ser	4420	2.5	1.8	3	4	—	—	—
α Boo	4375	1.6	1.6	2	—	—	—	—
HD 121447	4000	1.0	2.2	—	—	65	69	38
HD 178717	4100	1.0	2.2	—	—	46	56	26
HR 337	3800	1.6	2.1	—	25	26	23	14
BD+06°2063	3550	0.5	2.0	—	62	49	32	33
HD 96360	3550	0.5	2.1	—	58	52	40	32
HR 4483	3450	0.8	2.0	—	51	56	53	38
HR 5226	3650	1.0	2.8	—	42	46	38	27
HR 5299	3450	0.9	2.6	—	54	56	52	36
HR 6146	3250	0.2	2.7	—	60	65	55	46
BD−13°4495	3600	0.8	2.3	—	32	40	28	22
BD+16°3426	3450	0.5	2.0	—	57	52	49	41
HD 189581	3500	0.5	2.1	—	45	47	40	30
HR 8775	3600	1.2	2.0	—	37	41	38	23
HR 1105	3550	0.9	2.0	—	51	55	54	36
HR 1556	3450	0.8	2.0	—	46	47	48	31
BD+48 1187	3200	0.0	2.5	—	111	115	118	95
HD 35155	3650	0.8	2.7	—	61	59	55	42
BD+14 1350	3000	0.0	2.9	—	94	108	101	75
HD 49368	3700	1.0	2.5	—	54	60	45	37
HD 58521	3200	0.0	2.3	—	76	85	88	68
HD 64332	3500	0.5	1.8	—	58	50	55	40
HR 3639	3200	0.0	2.5	—	72	80	71	59
HR 4647	3450	0.5	1.8	—	65	58	55	44
BD−02°3726	3700	1.0	2.4	—	47	48	—	28
BD+57°1671	3600	0.8	2.2	—	44	45	40	31
BD−18°4320	3600	0.8	2.4	—	44	41	32	25
HR 6702	3300	0.7	2.5	—	62	63	63	46
HD 172804	3400	0.3	2.9	—	96	83	93	75
HD 199799	3400	0.3	1.7	—	74	80	77	57
HR 8062	3450	0.7	1.9	—	55	61	50	40
HD 44544	3500	0.0	3.1	—	—	—	172	142
HD 198164	3750	0.0	3.0	—	—	—	154	99
HD 209890	3000	0.0	2.9	—	—	—	182	120
HDE 286340	3500	0.0	3.0	—	—	—	201	122
AQ Sgr	2650	0.0	2.3	—	—	—	141	99
BL Ori	2860	0.0	2.0	—	—	—	131	92
R Lep	2390	0.0	1.6	—	—	—	115	90
R Scl	2550	0.0	1.9	—	—	—	127	101
RT Cap	2620	0.0	2.3	—	—	—	137	92
RV Cyg	2600	0.0	2.3	—	—	—	139	94
RY Dra	2500	0.0	2.4	—	—	—	131	79
S Sct	2895	0.0	2.2	—	—	—	136	105
ST Cam	2800	0.0	2.3	—	—	—	149	106
T Lyr	2380	0.0	2.6	—	—	—	137	79
TU Gem	2770	0.0	2.2	—	—	—	139	115
TW Oph	2450	0.0	2.2	—	—	—	131	81
TX Psc	3030	0.0	2.2	—	—	—	146	93
U Cam	2530	0.0	2.5	—	—	—	149	89
UU Aur	2825	0.0	2.3	—	—	—	145	105
UX Dra	2900	0.0	2.2	—	—	—	122	93
V Aql	2610	0.0	2.0	—	—	—	130	85

Table 3 (continued)

Star	$T_{\rm eff}$ (K)	log g	ξ (km s^{-1})	HF (1–0) equivalent widths in cm^{-1} 10^{-3}				
				R9	R13	R14	R15	R16
V460 Cyg	2845	0.0	2.2	—	—	—	130	87
V Hya	2650	0.0	1.5	—	—	—	—	65
VY UMa	2855	0.0	2.2	—	—	—	155	108
W CMa	2880	0.0	2.3	—	—	—	141	96
W Ori	2680	0.0	2.4	—	—	—	121	77
WZ Cas	2850	0.0	2.2	—	—	—	170	132
X Cnc	2620	0.0	2.1	—	—	—	156	113
Y Hya	2770	0.0	2.1	—	—	—	166	84
Y CVn	2730	0.0	2.4	—	—	—	119	65
Y Tau	2600	0.0	2.3	—	—	—	140	79
Z Psc	2870	0.0	1.8	—	—	—	138	86

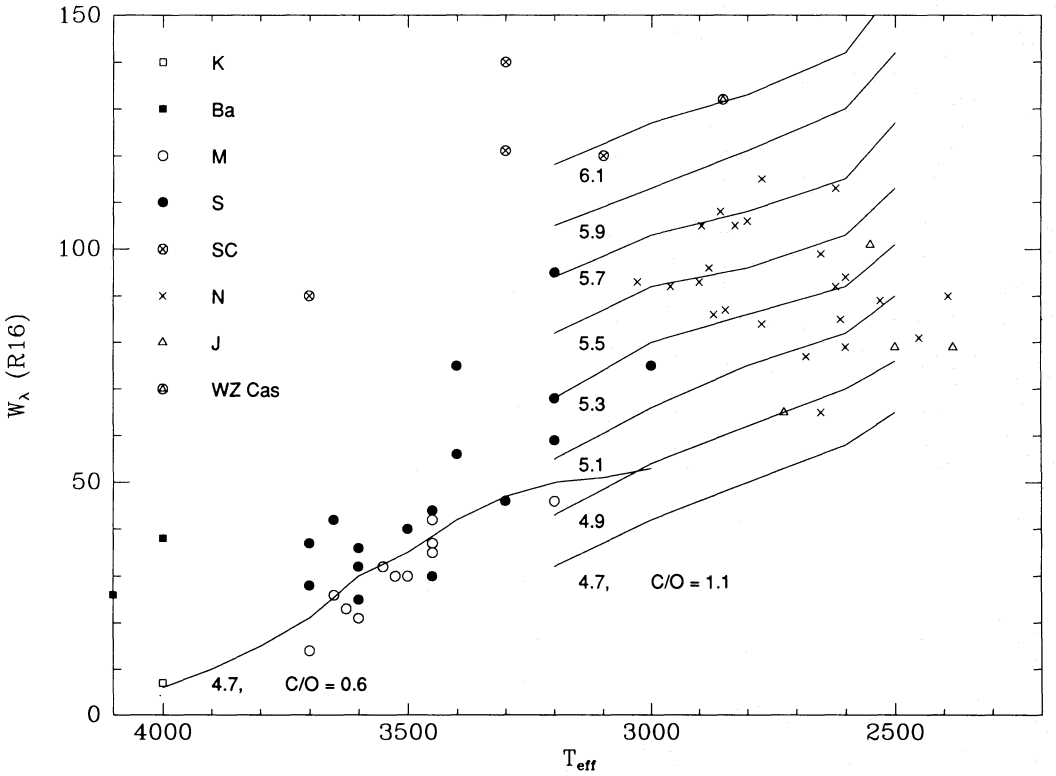

Fig. 3. Equivalent widths of the R16 line (in cm^{-1} 10^{-3}) as a function of $T_{\rm eff}$ for various samples of red giants. Predicted equivalent widths from model atmospheres are indicated by the solid lines for different F abundances, with each line labelled with the appropriate log ε(F) on the scale log ε(H) = 12.0. For the O-rich models, model atmospheres with C/O = 0.6 from Johnson et al. (1980) were used, while the C-rich models had C/O = 1.1 and were from Lambert et al. (1986), and both sets had log g = 0.0 with ξ = 2.3 km s^{-1}. The uncertainty introduced by the possible mismatch of the actual C/O ratio with that of the model should not be larger than 0.3 dex, as seen from the region of overlap between the two sets of models

the star's primordial envelope (Anders & Grevesse 1989), the ^{18}O(p, α)/^{18}O(p, γ) branching ratio quoted above acting on the ^{18}O primordial content is insufficient to build up a significant "^{19}F peak" in the envelope, as is the case for ^{13}C. Moreover, in deeper layers such that $\tau_{p\alpha}$ (^{19}F) < τ_{ms} (where $\tau_{p\alpha}$ (^{19}F) is the ^{19}F lifetime against ^{19}F(p, α)^{16}O and τ_{ms} is the star main sequence lifetime), ^{19}F will have been destroyed by the end of the main sequence lifetime.

From the relative values of the ^{14}N(p, γ)^{15}O, ^{16}O(p, γ)^{17}F, and ^{19}F(p, α)^{16}O cross sections (CF88), one may infer that the depletion of ^{19}F in the envelope starts at depths intermediate between the rise of the ^{14}N abundance and the ^{17}O peak in a

Table 4. Abundances

	$\log \varepsilon(^{19}F)$	[F/O]	$[\bar{M}/H]^e$	$[\Sigma CNO/\bar{M}]$	$[\Sigma' CNO/\bar{M}]$	$^{12}C/^{13}C^d$
K giants						
γ Dra	4.68	0.09	−0.23	0.06	−0.04	13
βUMi	4.52	−0.13	−0.23	0.11	0.05	11
α Ser	4.59	−0.11	−0.07	0.04	0.01	14
α Boo	4.01	−0.53	−0.56	0.26	0.17	7
Barium stars						
HD 121447	5.35	0.78	−0.21	0.21	0.06	8
HD 178717	5.24	0.77	−0.43	0.37	0.23	8
M and Stephenson's M stars						
HR 337	4.67	0.08	−0.09	0.01	−0.01	11
BD+06°2063[a]	4.77	0.37	−0.12	−0.03	−0.06	20
HD 96360[a]	4.76	0.12	−0.37	0.33	0.22	13
HR 4483	4.79	0.19	0.04	−0.08	−0.06	18
HR 5226	4.79	0.02	0.01	0.06	0.07	12
BD−13°4495[a]	4.51	0.08	0.02	−0.10	−0.09	12
BD+16°3426[a]	4.80	0.26	−0.11	0.04	0.01	16
HD 189581[a]	4.53	0.02	−0.30	0.16	0.07	15
HR 8775	4.64	0.06	−0.11	−0.01	−0.04	8
MS and S stars						
HR 1105	4.90	0.41	−0.07	0.01	−0.01	25
HR 1556	4.71	0.19	−0.11	0.00	−0.02	18
BD+48°1187	5.55	0.98	0.07	0.31	0.31	5
HD 35155	5.00	0.43	−0.53	0.39	0.19	8
BD+14°1350	5.28	0.79	na	0.29	na	30
HD 49368	4.99	0.42	−0.21	0.18	0.10	14
HD 58521	4.71	0.32	−0.18	0.10	0.03	43
HD 64332	4.78	0.19	−0.25	0.22	0.12	18
HR 3639	4.69	na	−0.17	na	na	50
HR 4647	4.80	0.25	−0.04	0.03	0.03	19
BD−02°3726	4.88	0.36	−0.17	0.08	0.01	16
HR 5299[b]	4.76	0.28	−0.12	−0.02	−0.05	9
BD+57°1671	4.76	0.25	−0.01	0.01	0.01	18
HR 6146[b]	4.61	0.08	−0.14	0.04	0.00	10
BD−18°4320	4.63	0.16	0.05	0.04	0.05	12
HR 6702	4.83	0.39	−0.08	−0.09	−0.10	20
HD 172804	4.97	0.70	0.23	−0.06	0.22	33
HD 199799	5.17	0.58	−0.19	+0.17	−0.14	28
HR 8062	4.75	0.28	−0.10	+0.06	−0.09	23
SC stars						
HD 44544	6.50	1.81	na	na	na	27
HD 198164	6.03	1.34	na	na	na	5.6
HD 209890	6.06	1.37	na	na	na	17
HDE 286340	6.20	1.51	na	na	na	30
N and J stars						
AQ Sgr	5.48	0.93	0.0	−0.04	−0.04	52
BL Ori	5.49	1.09	−0.1	−0.06	−0.09	57
R Lep	4.92	0.25	0.2	−0.13	−0.07	62
R Scl	5.40	1.30	na	na	na	19
RT Cap	5.31	0.81	−0.01	0.02	−0.01	59
RV Cyg	5.33	0.80	0.0	−0.03	−0.03	74
RY Dra	4.92	0.61	na	na	na	3.6
S Sct	5.70	1.12	−0.1	0.09	0.06	45
ST Cam	5.66	1.20	−0.1	0.01	−0.02	61
T Lyr	4.80	0.61	0.3	−0.66	−0.57	3.2

Table 4 (continued)

	$\log \varepsilon(^{19}F)$	[F/O]	$[\bar{M}/H]^c$	$[\Sigma CNO/\bar{M}]$	$[\Sigma' CNO/\bar{M}]$	$^{12}C/^{13}C^d$
TU Gem	5.80	1.47	na	na	na	59
TW Oph	4.91	0.49	0.3	−0.44	−0.35	65
TX Psc	5.55	0.96	−0.4	0.39	0.26	43
U Cam	5.12	0.85	−0.4	−0.47	−0.41	97
UU Aur	5.64	1.13	0.2	−0.24	−0.18	52
UX Dra	5.49	1.01	−0.2	0.10	0.04	32
V Aql	5.16	0.67	0.1	−0.17	−0.14	82
V460 Cyg	5.33	0.96	0.1	−0.29	−0.26	61
V Hya	4.86	0.22	0.1	−0.05	−0.02	69
VY UMa	5.72	1.32	0.1	−0.28	−0.25	44
W CMa	5.51	1.02	0.3	−0.38	−0.29	53
W Ori	5.07	0.73	0.0	−0.21	−0.21	79
WZ Cas	6.20	1.44	0.0	−0.16	−0.16	4.5
X Cnc	5.69	1.25	−0.3	0.16	0.07	52
Y Hya	5.23	0.76	−0.1	0.07	0.04	82
Y CVn	4.90	0.61	0.0	−0.26	−0.26	3.5
Y Tau	5.06	0.56	0.0	−0.08	−0.08	58
Z Psc	5.32	0.86	−0.1	−0.04	−0.07	55

[a] Stephenson's M star (Smith & Lambert 1990)
[b] s-process-rich M star (Smith & Lambert 1990)
[c] $[\bar{M}/H] = ([Ti/H] + [Fe/H] + [Ni/H])/3$; from Smith & Lambert 1990 for M, MS, and S stars; from Lambert & Ries 1981 for K stars.
[d] $^{12}C/^{13}C$ ratios from Lambert & Ries 1981, Smith 1984, Smith & Lambert 1990, Dominy et al. 1986, and Lambert et al. 1986.

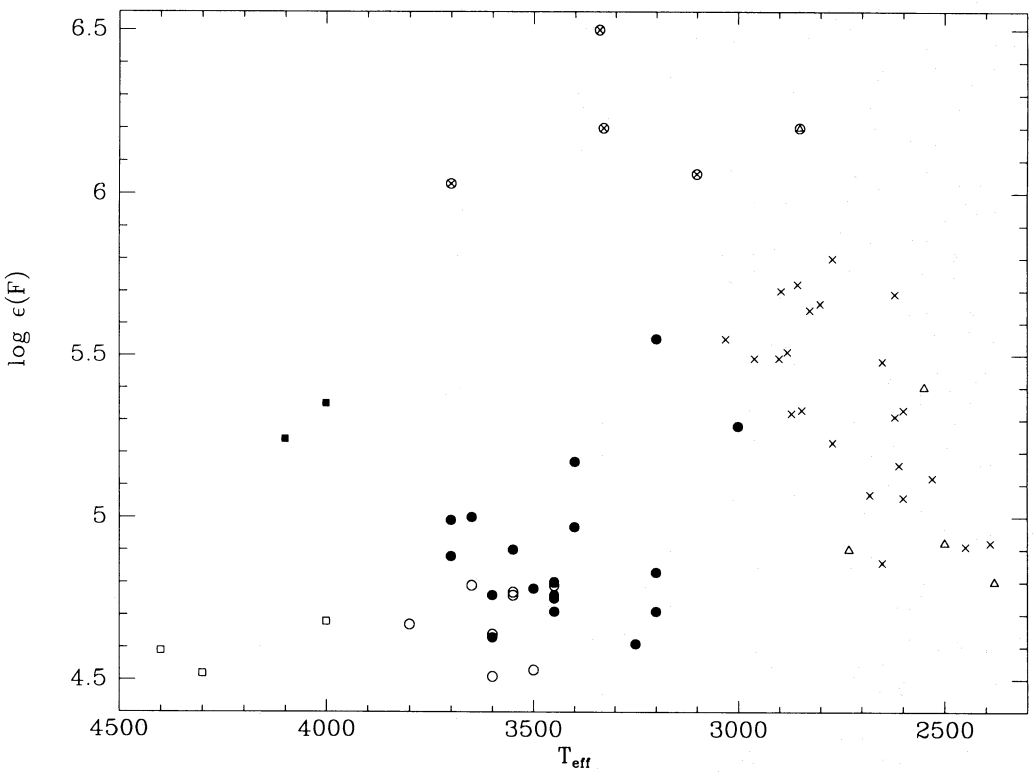

Fig. 4. Fluorine abundances, $\log \varepsilon(F)$, as a function of effective temperature for the various samples of red giants. The symbols are the same as in Fig. 3

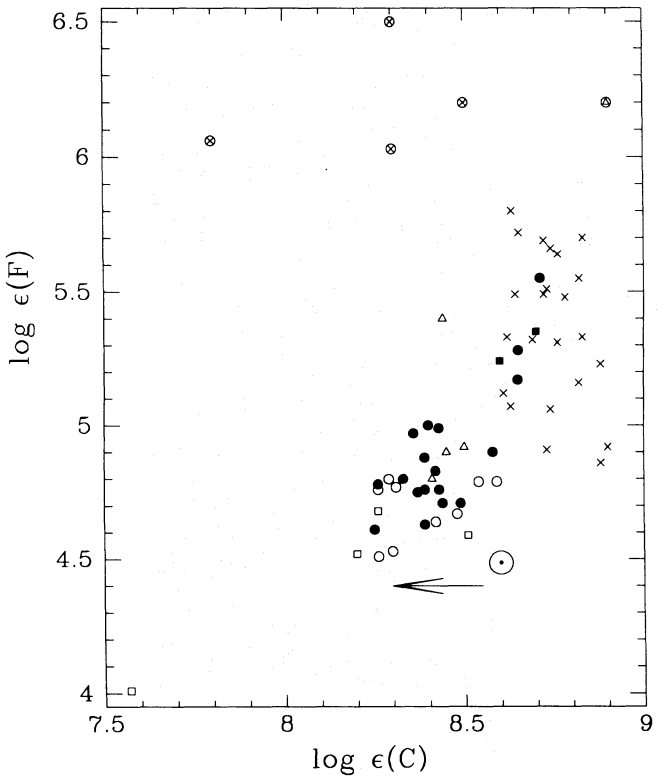

Fig. 5. Fluorine abundance log ε(F), versus carbon abundance, log ε(C): symbols have the same meaning as in Fig. 3. The solar symbol refers to the solar system abundance from Anders & Grevesse (1989). The arrow illustrates the approximate effect of the first dredge-up

main sequence star. In a $2M_{\odot}$ star (Dearborn et al. 1976), depletion begins at a depth of $M_r \sim 0.2M_{\odot}$. In that star, a dredge-up reaching the ^{17}O peak extends down to $M_r \sim 0.12M_{\odot}$, and such a dredge-up would then dilute ^{19}F by a factor $(2-0.2)/(2-0.12)=0.96$, inducing a reduction of the surface F abundance by only -0.02 dex. Since the first dredge-up is unlikely to extend to the ^{17}O-peak, the depletion may be even smaller. During the second dredge-up occurring in $M \gtrsim 4.5M_{\odot}$ stars at the end of core He-burning, the dilution of F deduced from Fig. 1 of Iben & Renzini (1983) for a $5M_{\odot}$ star is 0.90, corresponding to a reduction of the surface F abundance by -0.04 dex. In Fig. 5, the first and second dredge-ups will thus simply shift the giants relative to their primordial composition by ~ -0.25 dex along the log ε_C axis, as indicated by the arrow.

To disentangle the effects of galactic chemical evolution on the F abundance from stellar evolutionary effects, one should consider a diagram similar to Fig. 5, but with both axes normalized by a species sensitive to the galactic chemical evolution only and not to the nucleosynthesis occurring on the AGB. Iron-group species and oxygen are two good candidates. We note that they are not equivalent, neither from the point of view of the chemical evolution (since [O/Fe] ~ -0.5 [Fe/H] for disk stars; e.g. Lambert 1987), nor from that of the abundance analysis. The determinations of metallicity on one hand, and ^{12}C, ^{16}O, and ^{19}F abundances on the other hand, are not identically sensitive to the model atmosphere, due to the fact that the ^{12}C, ^{16}O, and ^{19}F abundances are not derived from atomic line-transitions; since uncertainties involved in the determinations of ^{12}C, ^{16}O, and ^{19}F abundances cancel to some extent, a normalization by oxygen appears to provide a better insight into the F overabundances than the normalization by metallicity. Indeed, the scatter resulting from the latter is much greater than the former. Of course, the assumption here is that the surface ^{16}O-abundance has not been measurably altered by high-temperature CNO cycling. Figure 6 shows the ([^{19}F/^{16}O], ^{12}C/^{16}O) plane, revealing a clear correlation between these two quantities (with the oxygen abundance from Lambert & Ries 1981; Lambert et al. 1986; Smith & Lambert 1990). Before addressing the implications of that correlation for AGB stellar models, we show that it is not an artifact of either the normalization nor the abundance analyses. Figure 7 shows that no obvious trend is present in the (log ε(O), ^{12}C/^{16}O) plane, hence the correlation between [^{19}F/^{16}O] and ^{12}C/^{16}O is not a result of the normalization by oxygen.

A spurious correlation of F with C/O might arise if a contribution from CN to the several HF lines has been overlooked. The HF R13 and R14 lines are blended with CN lines, while the R9, R15, and R16 lines used in the analysis appear unblended and a check against our thorough ^{12}CN and ^{13}CN linelists reveals no likely candidates. Moreover, the three unblended lines yield consistent F abundances. Other evidence against a major CN contribution to the HF lines is provided by the Barium and SC stars and the comparison of the ^{13}C-rich (J-type) and ^{13}C-poor cool carbon stars. Three J-type carbon stars show a lower F abundance than the average carbon star of much lower ^{13}C content, but the CN lines in the two types of stars have similar strengths and, of course, the ^{13}CN lines are much stronger in the J-type stars. Contamination by CN lines is thus unlikely to be the origin of the observed correlation. A systematic error tied to effective temperature can be rejected: Figure 4 shows that *high* F abundances are found among both hot and cool giants – HD 121447 is a late-K barium star with a F content as high as that of the S5 star HD 172804. Finally, the fact that the transition in F abundance from S to N stars is smooth, in spite of their rather different atmospheric structures and molecular chemical equilibrium both controlled by their C/O ratio, is another argument in favor of the reality of the ([^{19}F/^{16}O], ^{12}C/^{16}O) correlation. The SC stars, which are believed to be transition objects between the S and N classes, having (generally[1]) C/O = 1.00 $\pm$ 0.01, occupy, however, a rather eccentric position, being more ^{19}F-rich than most of the N stars. It should be mentioned that of all the stars studied, the SC stars may be the most affected by systematic differences between the model atmosphere and the real stars due to the very low boundary temperatures found in the C = O atmospheres (Johnson 1982).

The [F/O] ratios displayed in Fig. 6 are expressed relative to the mean value log $\varepsilon_F = 4.69 \pm 0.09$ of the 5 K and (genuine) M stars with [Fe/H] ≥ -0.20 from Table 4 (where the quoted uncertainty refers to the r.m.s. deviation) rather than to the meteoritic value. This mean stellar value is consistent with the solar photospheric value of 4.56 ± 0.30 obtained by Hall & Noyes (1969) using the HF lines in sunspots. However, our mean value for K and M giants is significantly higher than the solar system value log $\varepsilon_F = 4.48 \pm 0.06$ (Anders & Grevesse 1989), which is based upon two meteoritic measurements. Although the formal uncertainty on this value is small, Anders & Ebihara (1982) earlier questioned the accuracy of these two measurements,

[1] RZ Peg is a SC star in the revised MK classification of Keenan & Boeshaar (1980), but Dominy et al. (1986) found C/O = 1.2.

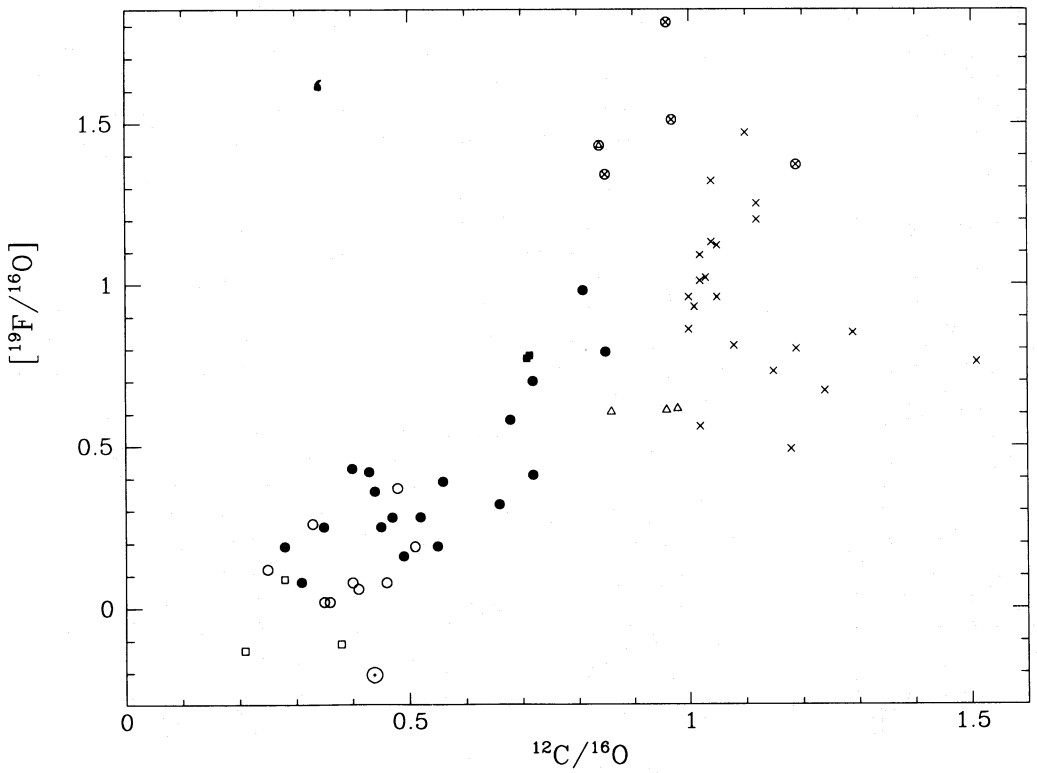

Fig. 6. The same as Fig. 5, with the abundances normalized by the ^{16}O abundance. Note that $[^{19}F/^{16}O] = (\log \varepsilon(^{19}F) - 4.69) - (\log \varepsilon(^{16}O) - \log \varepsilon_{\odot}(^{16}O))$ was not normalized by the solar system fluorine abundance ($\log \varepsilon_{\odot}(F) = 4.48$), but by the mean F abundance, $\log \varepsilon(F) = 4.69$, in K and M stars with $[Fe/H] \geq -0.20$

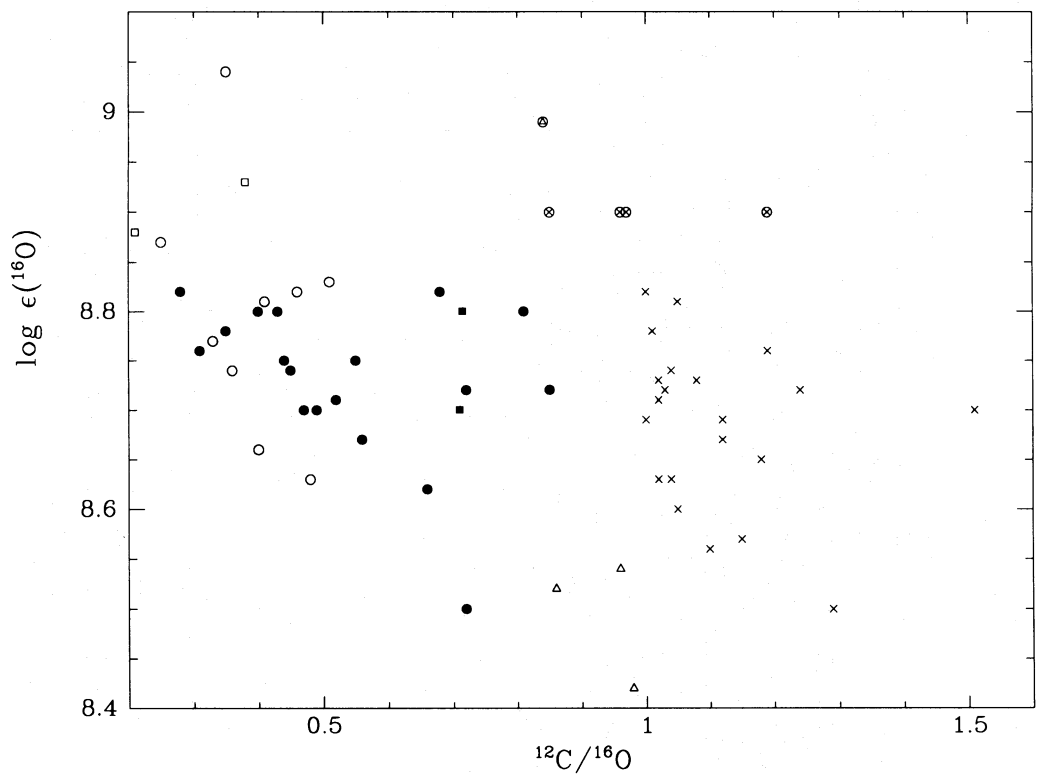

Fig. 7. Oxygen abundances in the various samples of red giants (see Fig. 3 for an explanation of the symbols) as a function of $^{12}C/^{16}O$. Since no large trend is apparent in the diagram, the normalization by ^{16}O cannot be responsible for the correlation ($[^{19}F/^{16}O]$, $^{12}C/^{16}O$) observed in Fig. 6

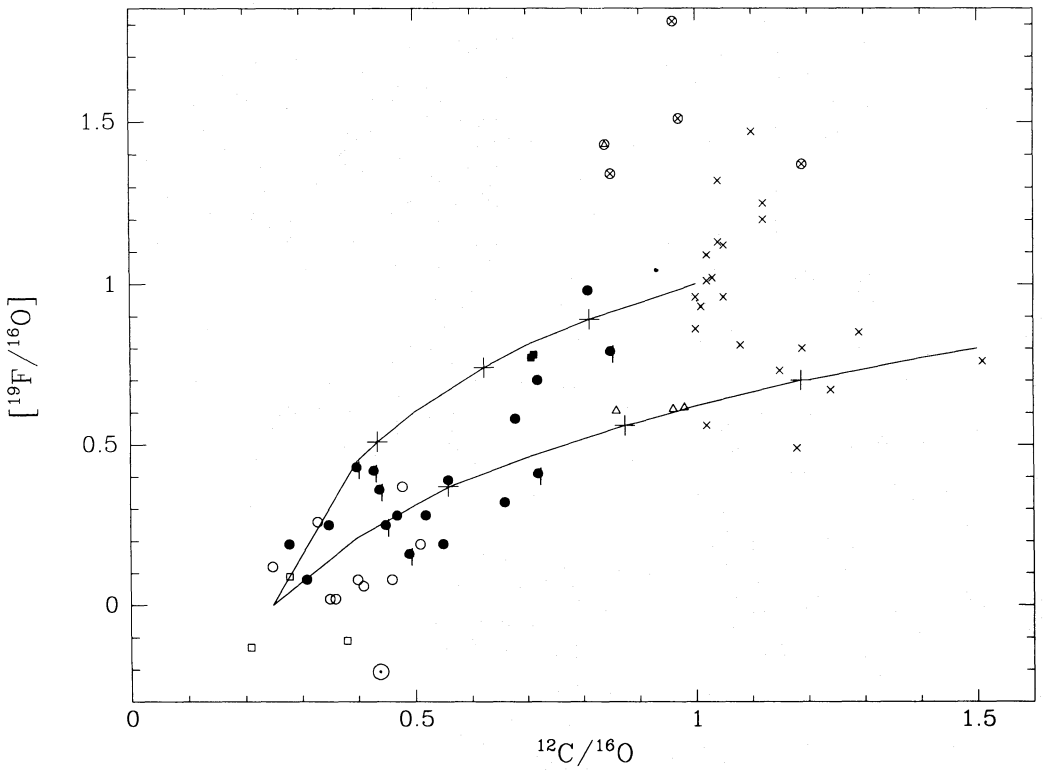

Fig. 8. Mixing lines representing the evolution of the envelope composition of extrinsic S stars as an increasing amount of material from an N star (upper-right end of the curve) is added to the envelope of a normal M star (lower-left end of the curve). The crosses on the mixing lines refer to dilution factors of 0.25, 0.50, and 0.75, respectively. Extrinsic S stars (without Tc) are identified by a vertical dash

warning that "the last word on F in meteorites has not yet been said". It seems possible that the discrepancy between the mean abundance of the K–M giants and the meteoritic log ε_F values may be due to uncertainties of the latter.

Another interesting feature of Fig. 6 concerns the relative location of extrinsic (non-Tc) and intrinsic (Tc) S stars. Intrinsic S stars are AGB stars where the heavy elements synthesized in their interior have recently been brought to the surface. As a consequence, Tc is still present in their envelope. In contrast, extrinsic S stars owe their peculiarities to mass transfer from a former AGB companion in a binary system and Tc is no longer present in their envelope. These extrinsic S stars are the likely descendants of the warmer barium stars (Brown et al. 1990). Both intrinsic and extrinsic S stars, as well as the barium stars HD 121447 and HD 178717, are seen to occupy the same region of Fig. 6, in agreement with the predictions of the mass transfer scenario for the barium and extrinsic S stars, as we now show. Mixing lines have been drawn in Fig. 8 for two different carbon star compositions. These lines describe the evolution of the surface abundance of F and C in an extrinsic S star when an increasing amount of matter from a carbon star is added to the envelope of a formerly normal M star, whose composition corresponds to the lower left end of the curve. The curves are labelled by the dilution factor $g = M_{acc}/(M_{acc} + M_{env})$, where M_{acc} is the amount of transferred matter from the N star envelope and M_{env} is the mass of the original, uncontaminated envelope. As can be seen in Fig. 8, the observed fluorine content of the N stars can thus easily account for the ^{19}F abundance of extrinsic S stars, provided that the dilution factor lies in the range 0.10–0.30 ($\sim$0.65 for BD+14°1350). These dilution factors are in quite good agreement with those deduced from the s-process abundances (Fig. 11 of Smith & Lambert 1990). This agreement[2] is encouraging, because it cannot only be regarded as a further argument in favor of the mass transfer scenario for extrinsic S (and barium) stars, but also as evidence that the abundances of ^{12}C, ^{19}F, and s-process elements in S and N stars are consistent with each other.

The similarity between the barium stars and the SC stars, pointed out by Dominy et al. (1986) on the ground of their C and O isotopic ratios (see also Wallerstein 1984), is confirmed in this work from the ^{19}F abundances. We also note that the carbon star

[2] Note that the peculiar position of HD 35155 in Smith & Lambert's Fig. 11, which would imply a dilution ratio of 0.7, is due to the abnormally high Nd abundance of that star: considering Zr instead of Nd would place HD 35155 among the other extrinsic S stars, so that a dilution factor in the range 0.1–0.3 would now be appropriate. The high dilution ratio required for BD+14°1350 from its high F content can unfortunately not be checked from the s-process abundances, which could not be determined in that star due to severe blanketing by molecular lines (Smith & Lambert 1990). This high dilution ratio might instead indicate that the internal nucleosynthesis processes responsible for the ^{19}F production in intrinsic S stars have begun to operate in BD+14°1350 and have already contributed to its surface ^{19}F abundance before that heavy element (Tc in particular) synthesis processes are themselves at work.

W CMa, which has been suggested to be a massive star ($M > 10 M_\odot$; Herbst et al. 1978; Scalo & Miller 1979), has a F abundance typical of C stars. If observations of F in red supergiants ($M > 10 M_\odot$) show that F is not enhanced in red supergiants, the suggestion that W CMa is a massive star can be rejected.

3.2. *Two constraints on the ^{19}F cooking site*

Figure 6 can be used to put two important constraints on the models of ^{19}F nucleosynthesis in AGB stars: it allows us to estimate both the amount of ^{19}F that has been brought into the envelope and the temperature at the ^{19}F cooking site. We first estimate the former by assuming that the mixing event responsible for the ^{19}F overabundance was also responsible for the increase of the envelope $^{12}C/^{16}O$ ratio, and that this mixing has no effect on the ^{16}O abundance. The pre-AGB fluorine abundance is assumed to be $\log \varepsilon_F = 4.69$ (see above). It is then possible to relate the abundances of ^{19}F and ^{12}C at the nucleosynthesis site independently of the dilution factor. In the case that the increase of F and $^{12}C/^{16}O$ observed in Fig. 6 results from a succession of mixings, this procedure, of course, only relates the *mean* value (over the many mixing events) of the ^{19}F amount in the nuclear processed matter to the *mean* ^{12}C content of that same matter.

In the following, the chemical symbols of nuclides without subscript will stand for their observed abundances in the stellar envelope, the subscript p identifies the abundances in the nuclear processed matter that contaminates the envelope, and the subscript e identifies the envelope abundances before contamination. The effect of the mixing can be expressed by the equations

$$\frac{^{19}F}{^{19}F_e} = (1-\gamma) + \gamma \frac{^{19}F_p}{^{19}F_e},$$

$$\frac{^{12}C}{^{12}C_e} = (1-\gamma) + \gamma \frac{^{12}C_p}{^{12}C_e},$$

where $\gamma = M_p/(M_p + M_e)$ is the dilution factor of the processed matter of mass M_p within the convective envelope of mass M_e. Eliminating γ between these two equations yields

$$\frac{^{19}F_p}{^{19}F_e} - 1 = \alpha \left(\frac{^{12}C_p}{^{12}C_e} - 1 \right), \qquad (1)$$

where $\alpha = (^{19}F/^{19}F_e - 1)/(^{12}C/^{12}C_e - 1)$ is entirely fixed by the observations. Lines of constant α in the plane ($[^{19}F/^{16}O]$, $^{12}C/^{16}O$) are presented in Fig. 9 (where it is assumed that ^{16}O is not altered in the process). These lines have in fact exactly the same shape as the mixing lines presented in Fig. 8. Equation (1) gives $^{19}F_p/^{19}F_e$ once $^{12}C_p/^{12}C_e$ is known. In the case that the mixing event under consideration corresponds to the third dredge-up, the mass fraction of ^{12}C in the nuclear processed matter should be in the range 0.2–0.3 (see e.g. Fig. 9 of Boothroyd & Sackmann 1988; Forestini et al. 1991). Assuming the 0.25 dex deficiency of C with respect to the solar system abundance (Anders & Grevesse 1989) found in normal, post-first dredge-up red giant envelopes, we adopt $^{12}C_p/^{12}C_e \sim 120$ (corresponding to

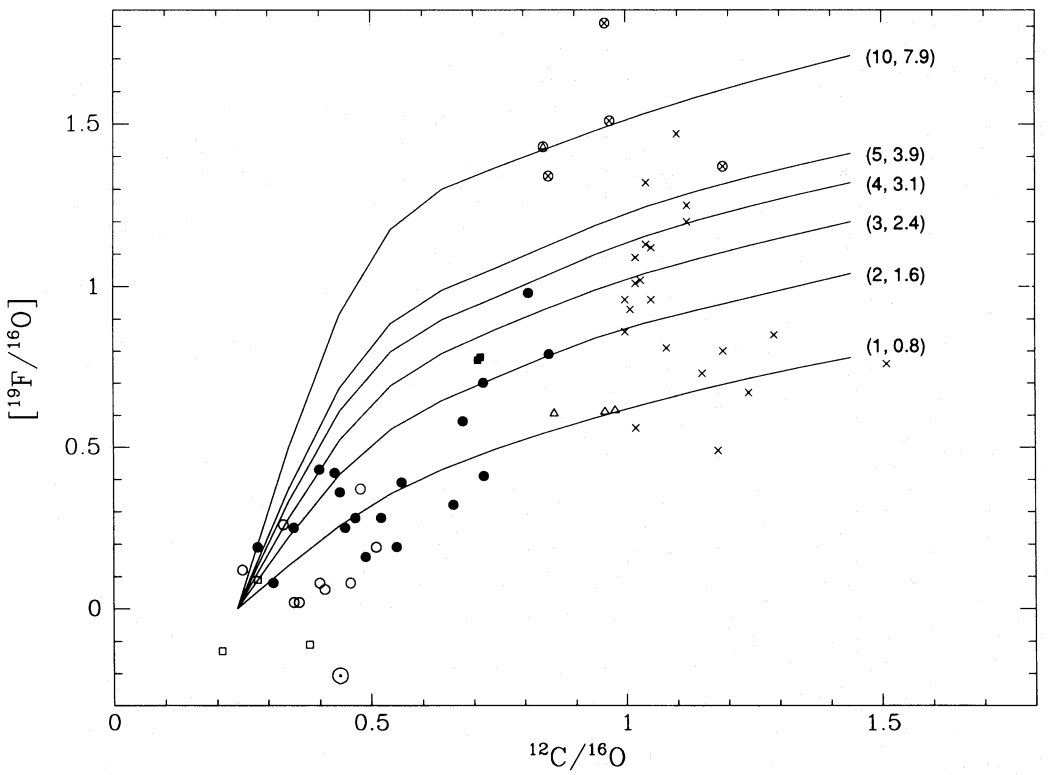

Fig. 9. Same as Fig. 6, where the curves correspond to a given mass fraction, $X_p(^{19}F)$, of ^{19}F in the dredged-up matter. The numbers along each curve give α (see text) and $X_p(^{19}F)$ (in units of 10^{-4}), respectively, for $^{12}C/^{16}O = 0.24$ and $X_e(^{19}F) = 6.6\,10^{-7}$ (or $\log \varepsilon(^{19}F) = 4.69$) in the red-giant envelope prior to the third dredge-up and $X_p(^{12}C) = 0.2$ in the dredged-up matter. For this choice of parameters, observations thus require that $0.8\,10^{-4} \lesssim X_p(^{19}F) \lesssim 8.0\,10^{-4}$. Adopting $X_p(^{12}C) = 0.05$, instead of 0.2, would decrease $X_p(^{19}F)$ accordingly

$X_p(^{12}C) = 0.2$), yielding the $^{19}F_p$ mass fraction listed along each curve in Fig. 9. In other words, most of the C and S stars of Figs. 6 and 9 require a mass fraction of ^{19}F in the nuclear processed matter of the order of $1\text{–}4\,10^{-4}$ if $X_p(^{12}C) = 0.2$, but the most enriched ones may require values as high as 10^{-3}. We emphasize that these values for $^{19}F_p$ correspond to our particular choice of $^{12}C_p$ and $^{12}C_e$ [see Eq. (1)].

The ability of various possible nucleosynthesis scenarios to produce the required ^{19}F mass fraction, $X_p(^{19}F)$, within AGB stellar models will be considered in Sect. 3.4.

We now consider ^{19}F as a thermometer and study the 11th pulse of a $7M_\odot$ star calculated by Iben (1982), for which the required data are available.

The ^{19}F lifetime against α capture, $\bar{\tau}_\alpha(^{19}F)$, has been computed as a function of time from the temperature and density profiles given in Fig. 7 in Iben (1982) for this particular pulse with $T_b = 286\,10^6$ K and $\rho_b = 3\,10^4$ g cm^{-3} (the temperature and density at the base of the convective shell). Since the $^{19}F(\alpha, p)^{22}Ne$ timescale is everywhere in the convective shell longer than the convective turnover time, $\bar{\tau}_\alpha(^{19}F)$ is taken as a mean value over the entire convective zone. This mean lifetime is 20 times longer than the lifetime at the base of the convective shell. Due to the rapid drop of temperature and density after the maximum extent of the convective shell, $\bar{\tau}_\alpha(^{19}F)$ varies strongly with time. It is thus useful to define the effective timescale, $\bar{\tau}_{eff}$, such that

$$X_{^{19}F}(\Delta t) = X_{^{19}F}(0)\exp(-\Delta t/\bar{\tau}_{eff}(\Delta t)),$$

with

$$\bar{\tau}_{eff}^{-1}(\Delta t) \equiv \frac{1}{\Delta t}\int_0^{\Delta t} \frac{dt'}{\bar{\tau}_\alpha(^{19}F, t')},$$

and $X_{^{19}F}(0)$ being the ^{19}F mass fraction at the time of the maximum extent of the convective shell. This effective timescale has been plotted on the lower panel of Fig. 10 as a function of time Δt after maximum extent of the pulse, and it appears that $\bar{\tau}_{eff} < \Delta t$, except for a very short period just after maximum. Due to the progressive retreat of the convective shell, a dredge-up depth, ΔM_d, will involve matter that was incorporated in the shell for a period of, at most, Δt (ΔM_d). Therefore, the line of slope 1 (i.e. $\Delta t = \bar{\tau}_{eff}$, corresponding to a 1/e reduction of the ^{19}F synthesized before maximum extension) in Fig. 10 can be parameterized in terms of $\lambda \equiv \Delta M_d/\Delta M_{csh}$ (where $\Delta M_{csh} \sim 3\,10^{-2} M_\odot$ is the maximum mass extent of the convective shell). This parameterization will be almost linear since the pulse shape is almost triangular. It reveals that dredge-up masses of $\Delta M_d \gtrsim 0.01\,\Delta M_{csh} \simeq 3\,10^{-4} M_\odot$ will be devoid of ^{19}F in Iben's model pulse.

For comparison, the same procedure has been applied to the 10th pulse of the $3M_\odot$ star (metallicity $Z = 0.01$, $\alpha = 1.5$) computed by Becker (1981) and the results are plotted on the upper panel of Fig. 10. Although this pulse is hotter ($T_b = 3\,10^8$ K and $\rho_b = 1.5\,10^4$ g cm^{-3}), the situation is not less favorable with respect to ^{19}F survival. This is due to the shorter duration of this pulse.

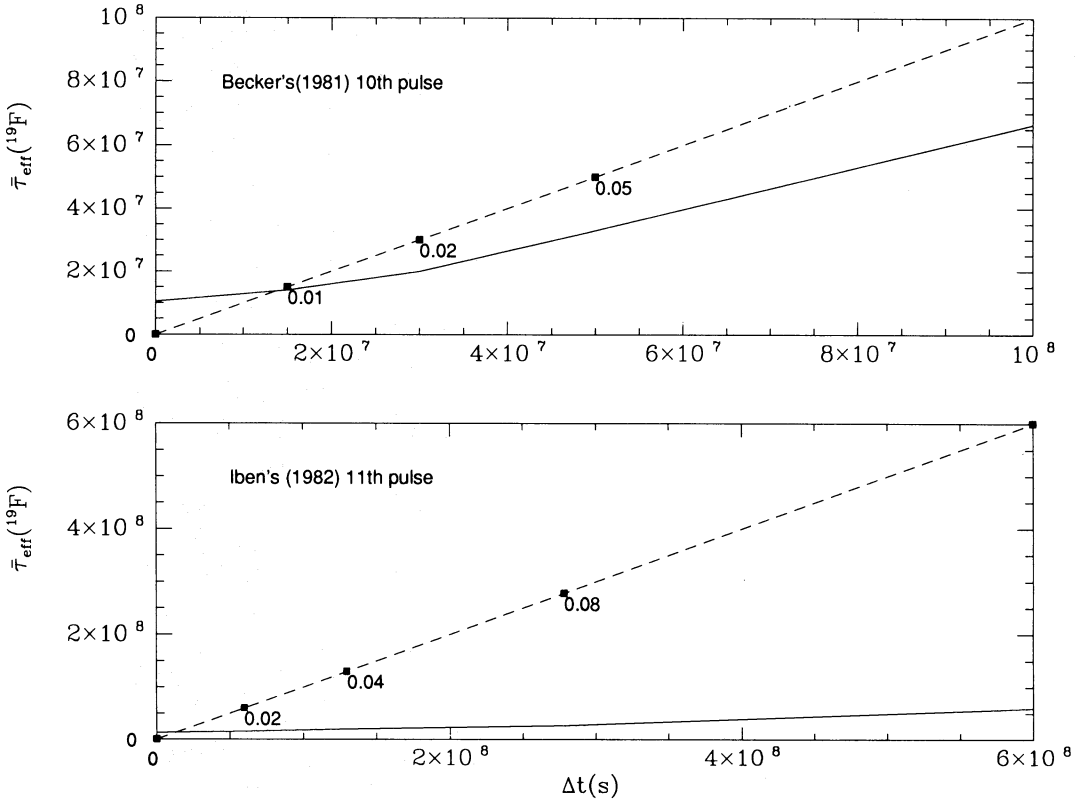

Fig. 10. The effective ^{19}F lifetime, $\bar{\tau}_{eff}(^{19}F)$ (in seconds), in the 10th thermal pulse of Becker (1981; upper panel) as a function of time after the maximum base temperature (solid curve). The line of slope 1 (dashed line), corresponding to $\bar{\tau}_{eff}(^{19}F) = \Delta t$, is parameterized in terms of $\lambda = \Delta M_d/\Delta M_{csh}$, where ΔM_d is the mass of material possibly dredged-up and ΔM_{csh} is the mass of the convective shell at maximum extension. Only when $\bar{\tau}_{eff}(^{19}F) \gtrsim \Delta t$ can the dredged-up matter be ^{19}F-rich

Figure 10 thus illustrates the sensitivity of the ^{19}F thermometer to the detailed properties of the thermal pulse. One may try to circumvent this sensitivity by using the timescale provided by the 3α reaction. We stated at the beginning of this section the rather general finding that partial He-burning during the thermal pulse leads to a final ^{12}C mass fraction of 0.2 to 0.3. We may thus compare the timescale needed by the 3α reaction to synthesize ^{12}C in the thermal pulse with the timescale for ^{19}F destruction. Overlap between successive pulses complicates somewhat that issue since ^{12}C from the ashes of one pulse will be engulfed into the next one. In the stationary regime established after a few pulses (as shown in Fig. 9 of Boothroyd & Sackmann 1988), it may be assumed that the 3α reaction is responsible for an increase of the ^{12}C mass fraction in the thermal pulse from 0.1 to 0.2. The former value results from a 50% dilution of the ashes of the previous pulse containing $X_p(^{12}C)=0.2$ within the following pulse.

Neglecting $^{12}C(\alpha,\gamma)^{16}O$, we calculate the timescale required by the 3α reaction to increase $X_p(^{12}C)$ from 0.1 to 0.2. The corresponding $\bar{\tau}_\alpha(^{12}C)\equiv 0.16\ \bar{\tau}_{3\alpha}(\alpha)$ and $\bar{\tau}_\alpha(^{19}F)$ timescales have been plotted on Fig. 11 as a function of T_b, for $\rho_b=10^3\ g\,cm^{-3}$ and $X_p(\alpha)=1$. Figure 11 thus shows that the requirement for simultaneous ^{12}C and ^{19}F dredge-up constrains the temperature of the thermal pulse: T_b may not greatly exceed $T\sim 3\,10^8$ K ($T_8\sim 3.0$). We emphasize that this value is rather poorly determined, not only because the slopes of the $\bar{\tau}_{3\alpha}(\alpha)$ and $\bar{\tau}_\alpha(^{19}F)$ curves are not very different, but also the critical temperature is quite sensitive to the adopted density (note that $\bar{\tau}_{3\alpha}\sim\rho^2$ while $\bar{\tau}_\alpha(^{19}F)\sim\rho$). Another factor affecting estimates of ^{19}F destruction is the $^{19}F(\alpha,p)^{22}Ne$ reaction rate which does not appear to be accurately known at the appropriate energies. The experimental investigation of Kuperus (1965) identifies resonant levels in the ^{23}Na compound nucleus for energies higher than 1.1 MeV above the $^{19}F+\alpha$ threshold, but no experimental information is available on the partial widths of resonant levels closer to the threshold that would be relevant in the $3.0\lesssim T_8\lesssim 3.5$ temperature range of interest here. The reaction rate provided by CF88 is identical to that of Woosley et al. (1978), who made use of a Hauser–Feshbach statistical algorithm. Since the level density is rather low (only 4 levels with the right spin and parity in the Gamow peak corresponding to $T_8=3$) and the α-widths are unknown, it is likely that the statistical estimate is uncertain by a factor 5–10 (Thibaud, private communication). A detailed investigation of this reaction rate in the energy range relevant for He-burning would clearly be of interest.

3.3. Does the ^{19}F overabundance in AGB stars rule out the operation of the $^{22}Ne(\alpha,n)^{25}Mg$ neutron source?

Under the assumption that the F and heavy-element synthesis are related events, the ratio of the $^{19}F(\alpha,p)^{22}Ne$ and $^{22}Ne(\alpha,n)^{25}Mg$ cross sections can be used to address the question of the possible operation of the $^{22}Ne(\alpha,n)^{25}Mg$ neutron source for heavy-element synthesis in AGB stars. From CF88, $^{22}Ne(\alpha,n)^{25}Mg$ appears to be at least 20 times slower than

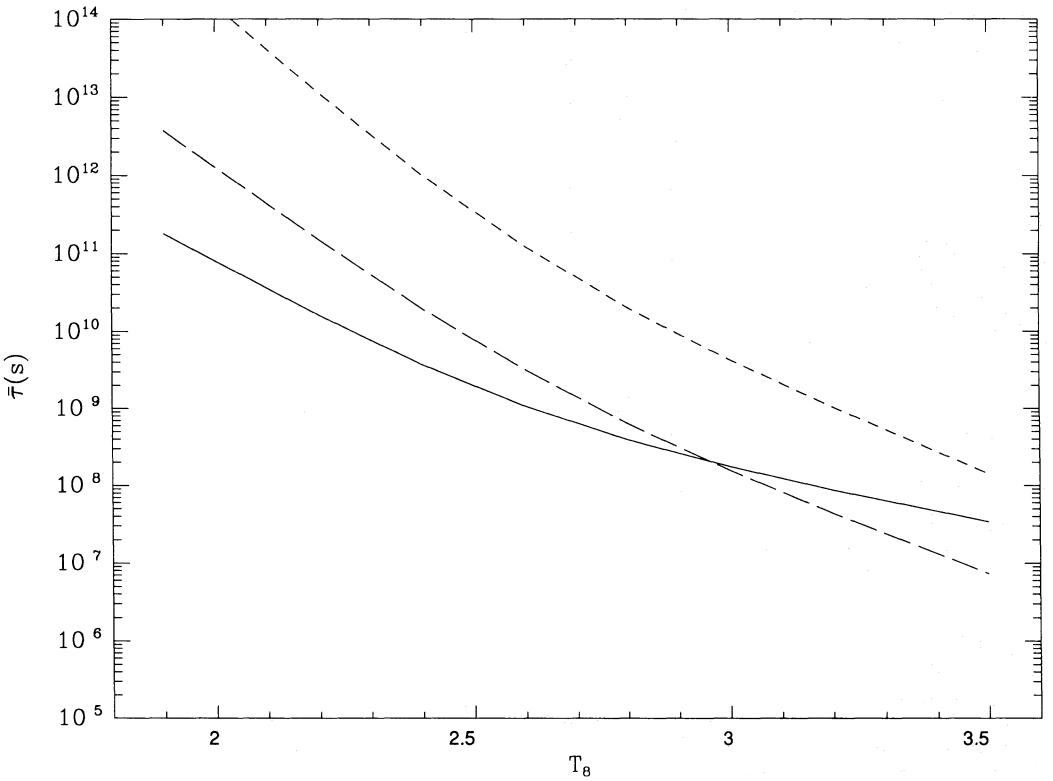

Fig. 11. Comparison of the timescale for ^{12}C synthesis, $\bar{\tau}(^{12}C)$, in the thermal pulse (solid curve; see text) with the lifetimes of ^{19}F, $\bar{\tau}_\alpha(^{19}F)$, (long dashed curve) and of ^{22}Ne, $\bar{\tau}_\alpha(^{22}Ne)$, (short dashed curve) against α captures, as a function of the base temperature and adopting $\rho=1000\ g\,cm^{-3}$ and CF88 reaction rates. Fluorine will not survive in pulses with base temperatures $T_8\gtrsim 3$ (as $\bar{\tau}_\alpha(^{19}F)\lesssim\bar{\tau}(^{12}C)$), although this value is sensitive to the adopted base density as well as to the uncertain $^{19}F(\alpha,p)^{22}Ne$ reaction rate

$^{19}F(\alpha, p)^{22}Ne$ in the $2.0 \lesssim T_8 \lesssim 3.5$ temperature range. Simultaneous neutron liberation by $^{22}Ne(\alpha, n)^{25}Mg$ and ^{19}F survival are therefore incompatible, at least from CF88 rates (see, however, Wolke et al. 1989; Drotleff et al. 1991 for a discussion of the nuclear uncertainties on the $^{22}Ne(\alpha, n)^{25}Mg$ cross section). The operation of the $^{22}Ne(\alpha, n)^{25}Mg$ neutron source would then clearly be ruled out by our observations of F overabundances.

Of course, the key assumption here is that ^{19}F and heavy-element synthesis occur in the same layers of AGB stars: this is far from being obvious. A first argument against this assumption may come from the large Maxwellian-averaged ^{19}F neutron capture cross section ($\langle\sigma\rangle = 5.4 \pm 1.1$ mb at 30 keV; Bao & Käppeler 1987). In consequence, ^{19}F will substantially be destroyed by $^{19}F(n, \gamma)^{20}F$ once the neutron exposure $\phi \gtrsim 1/\langle\sigma\rangle \sim 0.18\ mb^{-1}$, as appears to be the case for heavy-element synthesis in S stars (Smith & Lambert 1990). However, this destruction can be avoided should $^{18}O(n, \gamma)^{19}O(\beta^-)^{19}F$ compensate for the losses by $^{19}F(n, \gamma)^{20}F$, but as discussed in Sect. 3.4.4, successfully replenishment requires both a large ^{18}O content and a large ^{18}O neutron-capture cross section.

The relation between F and heavy-element synthesis is addressed from the observations in Fig. 12, which presents [F/O] versus [s/Ti], where [s/Ti] stands for the mean value of [Y/Ti], [Zr/Ti], and [Nd/Ti] abundances as provided by Smith & Lambert (1985, 1986, 1990) for the M, MS, and S stars, and by Utsumi (1985) for the N stars. The s-process abundances of the K giants and the J-type carbon stars were assumed to be solar (except for WZ Cas, which is not plotted and which has also been classified sometimes as an SC star; Keenan & Boeshaar 1980). There is a general trend for [F/O] to increase with [s/Ti]. Note that over the interval of $0.1 \leq [s/Ti] \leq 1.0$ and $0.0 \leq [F/O] \leq 0.5$ the S stars are scattered: this scatter is larger than the observational uncertainties, and is an indication that heavy-element synthesis and fluorine synthesis are not necessarily tightly related events, at least for the bulk of the S stars with $[F/O] \leq 0.5$. A clue to the question of the simultaneity of these synthesis events could perhaps be provided by the fluorine abundance of pure M stars with Tc, since these stars are believed to be in the early stage of heavy-element synthesis (see, however, Lattanzio & Malaney 1989). High fluorine overabundances in J stars provide a further hint that these two events are unrelated, since J stars are generally not s-process enriched (Utsumi 1985; Dominy 1985).

Nonetheless, for the most F-rich S and N stars, [F/O] and [s/Ti] are clearly increasing simultaneously. If this trend really indicates that fluorine and heavy-element synthesis are occurring together in AGB stars, the $^{22}Ne(\alpha, n)^{25}Mg$ neutron source can be ruled out because ^{19}F would be destroyed by $^{19}F(\alpha, p)^{22}Ne$ while neutrons are being liberated by $^{22}Ne(\alpha, n)^{25}Mg$.

3.4. An overview of potential nuclear paths of ^{19}F synthesis in AGB stars

In the context of He-burning (He-b) or combined H-He-burning (HHe-b, i.e. mixing of protons in a He-burning zone; see Hollowell & Iben 1989; Jorissen & Arnould 1989) relevant to AGB models, several nuclear reaction paths can be invoked for producing ^{19}F. We will briefly evaluate the respective merits of each of them from general arguments, trying to elucidate their properties

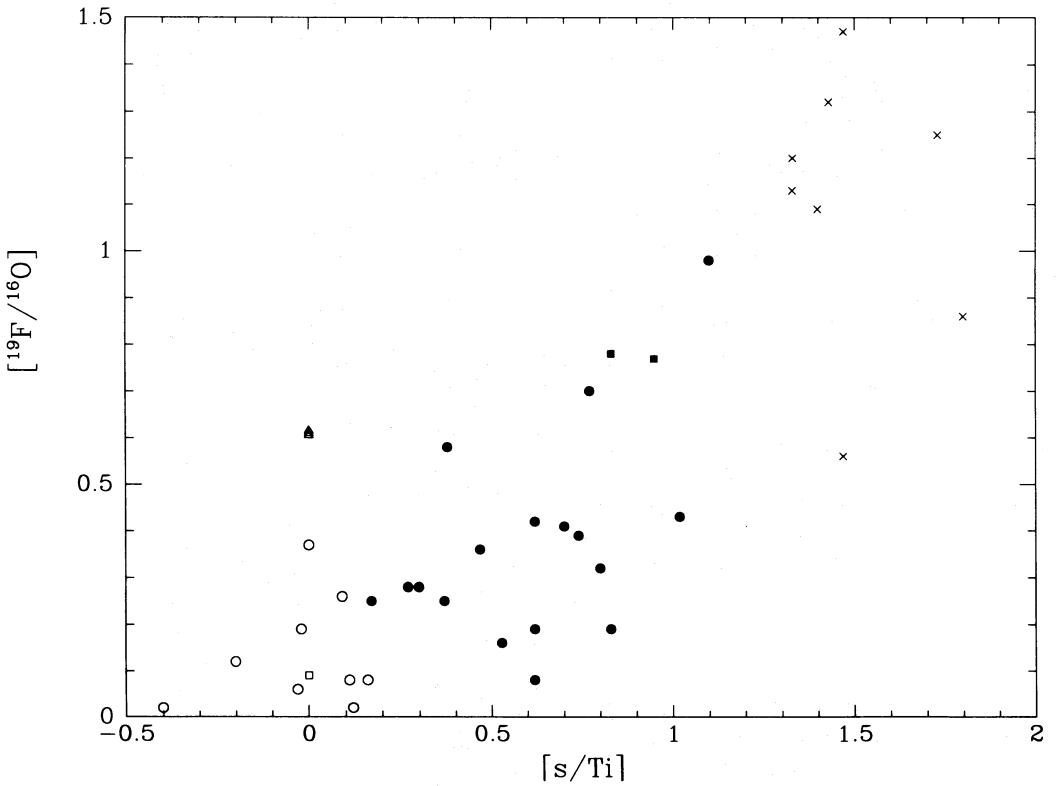

Fig. 12. Fluorine abundances versus the heavy-element abundances. The symbols are the same as in Fig. 3. [s/Ti] is defined as the mean value of [Y/Ti], [Zr/Ti], and [Nd/Ti]. For the K and J stars, the heavy-element abundances were assumed to be solar

independently of a particular stellar model. A discussion of the F nucleosynthesis in thermal pulses of a $3M_\odot$ AGB star, based on detailed stellar evolution calculations, is presented in a companion paper (Forestini et al. 1991; Paper I).

All[3] these nuclear paths involve $^{15}N(\alpha,\gamma)^{19}F$ as the last step, but ^{15}N production can be achieved in many different ways during He-burning or HHe-burning. The ^{15}N synthesis and its subsequent conversion into ^{19}F may be seen as two separate processes, due to the very different timescales involved.

Neutron captures will be seen to play an important role in ^{19}F synthesis. These neutrons are released either by $^{13}C(\alpha,n)^{16}O$ in the early phase of the burning process or by $^{18}O(\alpha,n)^{21}Ne$ at later phases if $T_8 \gtrsim 3$. In the former case, ^{13}C is made either as an ash of the previous CNO cycle operation, or by $^{12}C(p,\gamma)^{13}N(\beta^+)^{13}C$ resulting from the mixing of protons into the He-burning zone (HHe-b). In the following, ^{13}C originating from the CNO ashes will be referred to as secondary ^{13}C, while any ^{13}C from HHe-b will be referred to as primary ^{13}C. In the case of secondary ^{13}C, the supply available at the onset of He-burning is a function of both the star's metallicity and the temperature at which the CNO cycles ran. In matter of solar composition exposed to the CNO cycles at $T = 60\,10^6$ K ($T_6 = 60$), $X(^{13}C) = 10^{-4}$ (where $X(i)$ designates the mass fraction of nuclide i). In the case of HHe-b, the ^{13}C supply is not limited by the primordial CNO content, but is mainly fixed by the $^{12}C/p$ ratio characterizing the mixing of protons into the He- and C-rich layer (Jorissen & Arnould 1989; Hollowell & Iben 1990). The $^{18}O(\alpha,n)^{21}Ne$ reaction complements the neutron production by $^{13}C(\alpha,n)^{16}O$ during He-burning at $T_8 \gtrsim 3$, because the $^{18}O(\alpha,n)^{21}Ne/^{18}O(\alpha,\gamma)^{22}Ne$ branching ratio gradually favors (α,n) as T increases. The ^{18}O production results from $^{14}N(\alpha,\gamma)^{18}F(\beta^+)^{18}O$, ^{14}N being the most abundant ash of the CNO cycles: $X(^{14}N) = 1.3\,10^{-2}$ results from the operation of the CNO cycles in matter of solar composition, independently of the temperature. In the case of HHe-b, the ^{14}N supply may be even higher, depending on the $^{12}C/p$ ratio at the time of mixing.

The $^{22}Ne(\alpha,n)^{25}Mg$ neutron source, also associated with He-burning at $T_8 \gtrsim 3$, plays no role for the ^{15}N production due to its late occurrence in the He-burning process. The operation of $^{22}Ne(\alpha,n)^{25}Mg$ indeed relies on the ^{22}Ne supply made available by the $^{14}N(\alpha,\gamma)^{18}F(\beta^+)^{18}O(\alpha,\gamma)^{22}Ne$ chain. Therefore, the ^{14}N and ^{18}O seeds for the ^{19}F synthesis are not present when $^{22}Ne(\alpha,n)^{25}Mg$ operates. Moreover, $^{22}Ne(\alpha,n)^{25}Mg$ is at least 20 times slower than $^{19}F(\alpha,p)^{22}Ne$ in the $2.0 \leq T_8 \lesssim 3.5$ temperature range, so that $^{19}F(\alpha,p)^{22}Ne$ would destroy ^{19}F while neutrons are being liberated by $^{22}Ne(\alpha,n)^{25}Mg$.

Although neutron captures are involved in most of the ^{19}F synthesis paths, we emphasize that ^{19}F synthesis and heavy-element synthesis are not necessarily linked. This is because the number of neutrons available for capture by ^{56}Fe is usually small in the considered situations, either because a strong neutron poison is present (e.g. $^{14}N(n,p)^{14}C$, $^{18}F(n,p)^{18}O$, and $^{18}F(n,\alpha)^{15}N$) or because the neutron supply is very limited, especially when $^{13}C(\alpha,n)^{16}O$ operating from the CNO ashes is invoked. Typically, $n_c < {}^{13}C/{}^{56}Fe \simeq 0.5$, where n_c is the number of neutrons captured by initial ^{56}Fe nucleus and $^{13}C \simeq 10^{-5}$ results from the operation of the CNO cycles at $T_6 = 60$ in matter of solar composition; in the following, the chemical symbol of a species will stand for its molar fraction $Y = X/A$, where X is the mass fraction and A the mass number. If primary ^{13}C is involved (HHe-b), large ^{19}F production and heavy-element synthesis may occur together – see, however, our earlier remarks on ^{19}F destruction by $^{19}F(n,\gamma)$. Finally, it should be mentioned that, for many of the nuclear paths discussed below, the initial ^{13}C supply acts as a limiting factor for the amount of ^{19}F that can be synthesized.

3.4.1. $^{14}N(n,\gamma)^{15}N(\alpha,\gamma)^{19}F$

Since ^{14}N resulting from the former CNO cycle is very abundant at the onset of He-burning as neutrons are liberated by $^{13}C(\alpha,n)^{16}O$ also operating from the CNO ashes, this is the most obvious path for ^{19}F synthesis. Proton poisoning by $^{15}N(p,\alpha)^{12}C$ may, however, inhibit the ^{19}F production. The key to the efficiency of this path lies in the $^{14}N(n,\gamma)^{15}N/^{14}N(n,p)^{14}C$ branching, with $^{14}N(n,p)^{14}C$ being about 10 times faster than $^{14}N(n,\gamma)^{15}N$ (Fowler et al. 1967; Brehm et al. 1989). Hence, about 10 protons are released by $^{14}N(n,p)^{14}C$ for each ^{15}N nucleus synthesized by $^{14}N(n,\gamma)^{15}N$. Unless other proton poisons are abundant, ^{15}N will capture some of these protons and will thus never accumulate. In other words, $^{14}N(n,\gamma)^{15}N(\alpha,\gamma)^{19}F$ can only contribute to ^{19}F synthesis as a minor branching of $^{14}N(n,{}^{14}C)p({}^{18}O,\alpha)^{15}N(\alpha,\gamma)^{19}F$ when ^{18}O is the main proton poison.

3.4.2. $^{14}N(\alpha,\gamma)^{18}F(\beta^+)^{18}O(p,\alpha)^{15}N(\alpha,\gamma)^{19}F$ with $^{13}C(\alpha,n)^{16}O$ and $^{14}N(n,p)^{14}C$

This path occurs naturally at the onset of He-burning when neutrons liberated by $^{13}C(\alpha,n)^{16}O$ are captured by $^{14}N(n,p)^{14}C$, releasing the proton necessary for $^{18}O(p,\alpha)^{15}N$. It thus requires both ^{13}C and ^{14}N to be available initially, which is always the case when the He-burning region previously went through the CNO cycles, as indicated in Sect. 3.4. Moreover, ^{14}N is required to be the main neutron poison. This path operates in the $3M_\odot$ AGB model studied in Paper I.

The initial composition of the convective shell developing during thermal pulses results from the mixing of matter enriched in ^{13}C and ^{14}N through H-b or HHe-b with the ashes of the previous pulse. These ashes are ^{12}C- and, sometimes, ^{18}O-rich, as discussed below. Let us first consider the case where these ashes are devoid of ^{18}O. Since no ^{18}O is present in the CNO ashes either, the very first protons liberated by $^{14}N(n,p)^{14}C$ in the thermal pulse will be captured by $^{12}C(p,\gamma)^{13}N$ or by $^{14}N(p,\gamma)^{15}O(\beta^+)^{15}N$, thus providing a quite straightforward way to synthesize ^{15}N. The ^{18}O abundance will, however, progressively increase due to its production by $^{14}N(\alpha,\gamma)^{18}F(\beta^+)^{18}O$, so that $^{18}O(p,\alpha)^{15}N$ will rapidly become the dominant proton poison. But each proton captured by ^{18}O then produces ^{15}N which is itself a strong proton poison. Protons liberated by $^{14}N(n,p)^{14}C$ are thus almost equally shared by ^{15}N and ^{18}O. Since the number of available protons is fixed by the initial ^{13}C supply, $^{13}C(0)$, this amount also constitutes an upper limit to the ^{15}N that can be produced. The same upper limit is set on the ^{19}F

[3] If one excludes $^{18}O(n,\gamma)^{19}O(\beta^-)^{19}F$ and $^{16}O(^3He,\gamma)^{19}Ne(\beta^+)^{19}F$, suggested by a possible link between Li and F synthesis: WZ Cas is indeed both a super Li-rich and super F-rich star (Wallerstein & Torres-Peimbert 1968; Denn et al., 1991). However, ^3He will be consumed much faster by ^4He, because of the smaller Coulomb barrier.

yield, because of the subsequent conversion of ^{15}N into ^{19}F by $^{15}N(\alpha,\gamma)^{19}F$. At optimum efficiency, $^{19}F = {}^{15}N \sim {}^{13}C(0)$, which can be reached only if $^{14}N(n,p)^{14}C$ is the main neutron poison and if $^{18}O(p,\alpha)^{15}N$ is the main proton poison. The former condition relies critically on the $^{14}N(n,p)^{14}C$ cross section, which is still uncertain (Brehm et al. 1989; Koehler & O'Brien 1989) and on the ^{14}N dilution factor from the H-burning ashes into the thermal pulse. Adopting Brehm et al.'s cross section ($\langle\sigma_{14}\rangle = 0.9$ mb at 30 keV) and a dilution factor of 0.5 (related to the "overlap factor" between successive pulses), the condition is marginally satisfied in solar metallicity stars, since $\langle\sigma_{14}\rangle^{14}N = 4.2\,10^{-4}$, but $\langle\sigma_{56}\rangle^{56}Fe = 2.7\,10^{-4}$. The Koehler & O'Brien cross section, which is about 2.5 times larger, would strengthen that inequality, with 80% of the available neutrons now being captured by $^{14}N(n,p)^{14}C$. On the other hand, a much smaller dilution factor (as is the case for the primary ^{14}N produced in the semiconvective scenario of Hollowell & Iben; see below) would violate the above inequality, making the ^{19}F synthesis much less efficient.

We examine now the requirement that ^{18}O be the main proton poison. When ^{18}O is initially abundant, as neutrons and protons are released, most protons are captured by ^{18}O and ^{15}N losses by protons are then avoided. The possibility that the $^{14}N(\alpha,\gamma)^{18}F(\beta^+)^{18}O(\alpha,\gamma)^{22}Ne$ chain may not go to completion[4] in early pulses of low temperature, leading to the accumulation of ^{18}O from one pulse to the other was pointed out by Thielemann & Arnould (1979) and confirmed by Boothroyd & Sackmann (1988; see especially their Fig. 10) and by Paper I from detailed pulse calculations. Since ^{18}O is then approximately equal to the ^{14}N supply from the CNO cycle ($^{14}N_{CNO}$), the assumption that proton captures by ^{18}O dominate those by ^{15}N translates into

$$\frac{^{18}O}{^{15}N} \gtrsim \frac{^{14}N_{CNO}}{^{13}C(0)} \gg \frac{\langle\sigma v\rangle_{15p\alpha}}{\langle\sigma v\rangle_{18p\alpha}},$$

since ^{15}N will at most reach the initial ^{13}C abundance. The equilibrium $^{14}N_{CNO}/^{13}C$ ratio resulting from the CNO cycles ranges from ~ 490 at $T_6 = 20$ to 80 at $T_6 = 80$ (CF88), while $\langle\sigma v\rangle_{15p\alpha}/\langle\sigma v\rangle_{18p\alpha}$ ranges from 0.43 to 6.6 for typical He-burning temperatures $1.5 \leq T_8 \leq 3.0$, so that most protons are captured by ^{18}O.

In summary, low-temperature pulses are a situation where the optimum efficiency of ^{19}F synthesis through the path $^{14}N(\alpha,\gamma)^{18}F(\beta^+)^{18}O(p,\alpha)^{15}N(\alpha,\gamma)^{19}F$ can be attained: first, ^{14}N from the CNO cycle or HHe-b is converted into ^{18}O by an α-capture, but the pulse temperature is too low or its duration too short to convert it into ^{22}Ne by another α-capture. Then, ^{18}O surviving that pulse is incorporated into the next one, and the protons released in the early phase of this pulse by $^{13}C(\alpha,n)^{16}O$ followed by $^{14}N(n,p)^{14}C$ convert ^{18}O into ^{15}N by $^{18}O(p,\alpha)^{15}N$; ^{15}N will ultimately be transformed in ^{19}F via $^{15}N(\alpha,\gamma)^{19}F$. At optimum efficiency this path yields $X_p(^{19}F) \sim 1.5\,10^{-4}$, assuming that $X(^{13}C) \sim 10^{-4}$ in the ashes from the CNO cycle operating at $T_6 = 60$ in matter of solar composition.

Even this optimum F production is only just able to account for the least F-enriched S stars in Fig. 9. A further problem with this scenario is that the envelope is not only enriched in ^{19}F, but also in ^{18}O, that is not totally consumed by $^{18}O(p,\alpha)^{15}N$ and $^{18}O(\alpha,\gamma)^{22}Ne$. For example, if $X_p(^{18}O) = 10^{-2}$ and $X_p(^{12}C) = 0.20$, a dilution factor of $5\,10^{-3}$ for the nuclear processed matter in the outer envelope leads to $^{12}C/^{16}O = 0.37$ (initially 0.24) and $^{16}O/^{18}O = 150$ (initially 500), as discussed in Paper I. Such a reduction of the $^{16}O/^{18}O$ is not observed in the S stars (Smith & Lambert 1990).

To match the observations, it seems thus necessary to invoke a primary ^{13}C production by HHe-b at the level $X_p(^{13}C) \sim 5\,10^{-4}$–$10^{-3}$ *after dilution within the thermal pulse.* A larger initial ^{13}C supply would indeed allow ^{19}F production at the level required by the observations even if the ^{19}F synthesis efficiency is not optimum, and would remove the need for a large initial ^{18}O content and the associated reduction of the surface $^{16}O/^{18}O$ ratio after dredge-up. We note that Hollowell & Iben's scenario for HHe-b is unable to meet the requirement on $X_p(^{13}C)$ expressed above, because high ^{13}C and ^{14}N abundances ($X \sim 0.02$) are only obtained in a very thin layer of a few $10^{-4} M_\odot$ which is ultimately diluted in the $\sim 10^{-2} M_\odot$ thermal pulse, so that the resulting $X_p(^{13}C)$ is only $\sim 2\,10^{-4}$. Moreover, the same dilution factor applied to ^{14}N makes $^{14}N(n,p)^{14}C$ unable to compete with $^{56}Fe(n,\gamma)$, a situation favorable for heavy-element synthesis, but one which inhibits the ^{19}F synthesis by cutting the proton supply necessary for $^{18}O(p,\alpha)^{15}N(\alpha,\gamma)^{19}F$. Nevertheless, observations seem to confirm the synthesis of the necessary ^{13}C (and concomitant ^{14}N) by HHe-b at least in S stars, as shown in Fig. 13. Figure 13 is a plot of $[^{19}F/^{16}O]$ versus $^{12}C/^{16}O$, where the size of the symbols is related to their "CNO excess" [ΣCNO/Fe] (see Smith & Lambert 1990). It should be noted, however, that galactic chemical evolution effects may lead to spurious values for the CNO excess, because $[O/Fe] \sim -0.5[Fe/H]$ in unevolved disk stars (e.g. Wheeler et al. 1989) with O being the dominant contributor to the sum. Therefore, when normalizing the CNO sum, the effective oxygen abundance $O' = O_\odot\ 10^{-0.5[Fe/H]}$ has to be used instead of the solar system value $O_\odot$. The CNO sum normalized in such a way is listed as $[\Sigma' CNO/\bar{M}]$ in Table 4.

Note that the $[\Sigma CNO/\bar{M}]$ values given by Smith & Lambert (1990) are in error; the correct values are listed in Table 4. Pollution of the envelope by nuclear processed matter through the CNO cycles operating on the stellar primordial CNO nuclei does not alter [ΣCNO/Fe], which should remain close to 0.0. Addition to the envelope of fresh ^{12}C from the 3α reaction or ^{14}N from the CN cycle operating on ^{12}C from 3α (HHe-b situations) will lead to an increase of [ΣCNO/Fe]. The observations reveal that $[\Sigma CNO/Fe] \gtrsim 0.1$ in several S stars, and a close look at the C, N, O abundances (Smith & Lambert 1990) shows that it is N that is responsible for the CNO excess. Quite interestingly, Fig. 13 reveals that the most F-rich S stars (for a given C/O ratio) are also those with $[\Sigma CNO/Fe] \gtrsim 0.1$, suggesting that the primary ^{13}C production, which is likely to be associated with the observed N excess, is able to trigger a larger ^{19}F production, in agreement with our nucleosynthesis models.

Such an N excess is not observed in the N stars, which are nevertheless very F-rich (see, however, Lambert et al. 1986, for a discussion of the uncertainties on the N abundances in these stars). In these stars, one may consider the feedback of the increased C content of the envelope on the ^{13}C yield from the H-burning shell. As the envelope is progressively enriched in C by the third dredge-up, the H-burning shell operating beneath the envelope will be fueled by more CNO-rich matter. The ashes of

[4] Remember that when no HHe-b is involved, $^{13}C(0) \ll {}^{14}N(0)$ so that $^{18}O(p,\alpha)^{15}N$, although of prime importance for ^{15}N synthesis, is a minor branching to $^{18}O(\alpha,\gamma)^{22}Ne$.

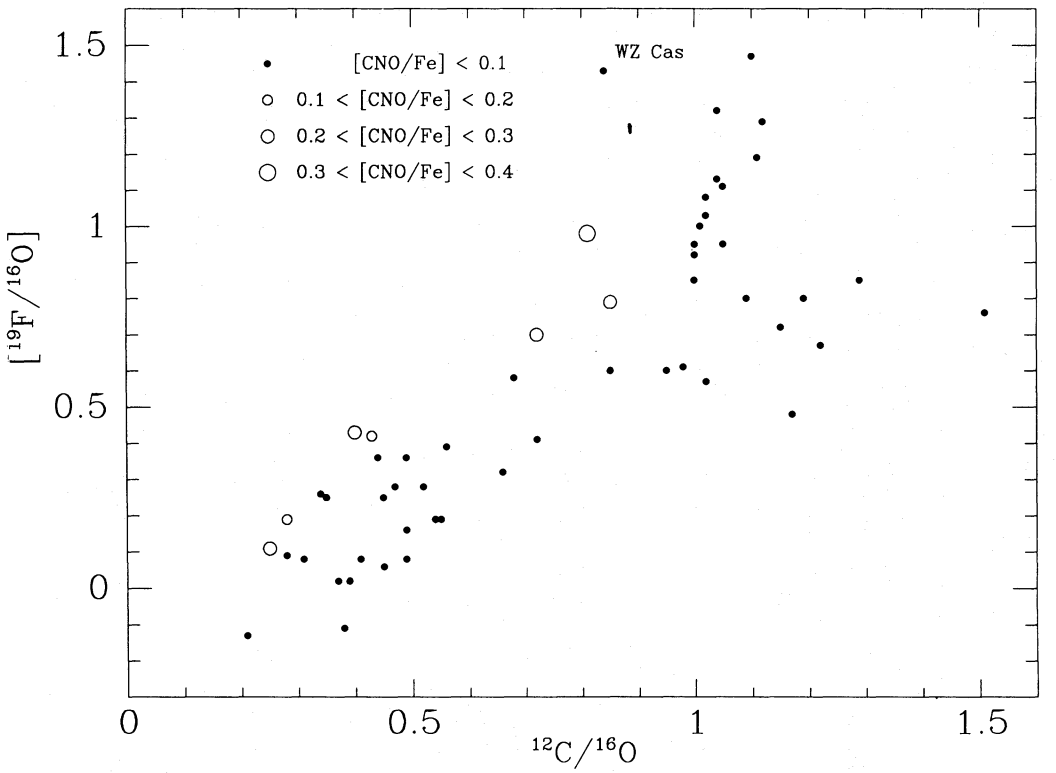

Fig. 13. Same as Fig. 6, except that stars with CNO excesses ([CNO/Fe] ≥ 0.1, where CNO stands for the sum of the corresponding nuclides, corrected for Galactic chemical-evolution effects; see text) are identified by open circles. Note that the stars with CNO excesses are the most F-rich for a given $^{12}C/^{16}O$ ratio

the CNO cycle may thus be expected to be proportionally enriched in ^{13}C. For example, when $^{12}C/^{16}O = 1.2$ in the envelope, the ^{13}C yield from the CNO cycle at $T_6 = 60$ will be increased by the same factor, thus amounting to $X(^{13}C) = 1.5\,10^{-4}$. Assuming that thermal pulses in carbon stars are cool enough to allow ^{19}F to survive the pulse, optimum ^{19}F synthesis efficiency leads to $X_p(^{19}F) = 2.2\,10^{-4}$, which is not yet large enough to account for the most F-rich N stars (Fig. 9). As indicated in Sect. 3.4.3, a possible way to cure the problem would be to invoke low-mass envelopes for N stars, so that $X_p(^{12}C)$ as small as 0.05 would be able to drive the surface $^{12}C/^{16}O$ ratio above unity. With such a low $X_p(^{12}C)$ value, ^{19}F overabundances in N stars can be accounted for with $X_p(^{19}F) \leq 2\,10^{-4}$ according to Eq. (1) and Fig. 9.

3.4.3. $^{14}N(\alpha,\gamma)^{18}F(\beta^+)^{18}O(p,\alpha)^{15}N(\alpha,\gamma)^{19}F$ and $^{14}N(\alpha,\gamma)^{18}F(n,\alpha)^{15}N(\alpha,\gamma)^{19}F$ with $^{18}O(\alpha,n)^{21}Ne$ and $^{18}F(n,p)^{18}O$

In the He shell, when $T_8 \gtrsim 3$ at $\rho = 10^3\,g\,cm^{-1}$, $\tau_\alpha(^{14}N) < \tau_\beta(^{18}F)$ and, therefore, ^{18}F accumulates before decaying. As the branching ratio $^{18}O(\alpha,n)^{21}Ne/^{18}O(\alpha,\gamma)^{22}Ne$ increases with temperature, $^{18}O(\alpha,n)^{21}Ne$ is efficient in the He-shell, and supplies neutrons that allow $^{18}F(n,p)^{18}O$ to act as a proton source. Then the ^{19}F synthesis follows as previously from $^{18}O(p,\alpha)^{15}N(\alpha,\gamma)^{19}F$. This path is slightly more efficient with the $^{18}O(\alpha,n)^{21}Ne$ neutron source than with $^{13}C(\alpha,n)^{16}O$ considered in Sect. 3.4.2. At $T_8 = 3$ and $\rho = 10^3\,g\,cm^{-3}$, $X_p(^{19}F) \sim 2.0\,10^{-4}$ is obtained when $^{14}N(0) = 9.3\,10^{-4}$ (ashes of CNO-cycling in solar composition matter).

Problems with this scenario are (i) the high temperatures involved, which make the destruction by $^{19}F(\alpha,p)^{22}Ne$ rather fast with respect to the 3α reaction (though the $^{19}F(\alpha,p)^{22}Ne$ rate is still uncertain), and (ii) the rather small amount of ^{19}F synthesized with respect to the observations.

Both problems can be circumvented by invoking a primary ^{14}N supply from HHe-b, since the efficiency of the ^{19}F synthesis is proportional to the initial ^{14}N supply. With a larger ^{19}F production, some destruction by $^{19}F(\alpha,p)^{22}Ne$ could then be tolerated. The observation of an N excess in the most F-rich S stars (at a given C/O ratio; Fig. 13) suggests that a primary ^{14}N production occurs in these S stars.

As indicated previously, such an N excess is not observed in the N stars, which are nevertheless very F-rich. For these evolved AGB stars, it is possible to invoke instead a small envelope mass. This requirement is consistent with the high pulse temperatures needed for this scenario, since both features are expected to be typical of evolved AGB stars – mass loss is likely to be heavy at the high luminosities of the most evolved AGB stars. Moreover, if the envelope mass is small, the increase of the surface C/O ratio can be achieved with smaller $X_p(^{12}C)$ in the dredged-up matter. For example, a 2% increase of the surface C/O ratio from 1 to 1.02 would require a dilution factor of $3.4\,10^{-3}$ if $X_p(^{12}C) = 0.05$ and $X_e(^{12}C) = 7.3\,10^{-3}$ when C/O = 1 (Lambert et al. 1986). If the dredged-up mass amounts to $\Delta M_p = 10^{-3} M_\odot$ (e.g. Lattanzio 1989), the envelope mass should then be $M_{env} \sim 0.3 M_\odot$. The advantage of adopting $X_p(^{12}C) = 0.05$ and a low M_{env} is that, according to Eq. (1) and Fig. 9, the same observed [F/O] overabundances require much lower $X_p(^{19}F)$ values than with $X_p(^{12}C) = 0.2$: all N stars then require $X_p(^{19}F) < 2\,10^{-4}$ (instead

of $8\,10^{-4}$ when $X_p(^{12}C)=0.2$) to account for the observed ^{19}F overabundance. These values are within the range that may be reached with the ^{14}N supplied by CNO-cycled ashes. There is thus no need for HHe-b to yield primary ^{14}N in N stars, in agreement with the observed lack of N excess in N stars (Lambert et al. 1986; Smith & Lambert 1990). It should be added that $X_p(^{12}C)=0.05$ in the dredged-up matter is also compatible with a short exposure of that matter to high temperatures, thus preventing ^{19}F destruction by $^{19}F(\alpha,p)^{22}Ne$. Such a small ^{12}C content in the thermal pulse may, however, contradict theoretical models (e.g. Boothroyd & Sackmann 1988, Fig. 9).

Inspection of Fig. 13 shows a large spread in the F abundances of N stars, but a modest range in the C/O ratios. The N stars with F overabundances larger than those of S stars, but with $^{12}C/^{16}O$ ratios close to unity ($^{12}C/^{16}O<1.1$), may have a low-mass envelope polluted by matter rich in F, but rather C-poor. On the other hand, N stars with F abundances similar to those found in the S stars, but higher $^{12}C/^{16}O$ ratios (1.0–1.5), may instead have higher-mass envelopes, and their F content can easily be accounted for by the scenario of Sect. 3.4.2.

3.4.4. $^{14}N(\alpha,\gamma)^{18}F(\beta^+)^{18}O(n\,\gamma)^{19}O(\beta^-)^{19}F$ with $^{13}C(\alpha,n)^{16}O$ and/or $^{18}O(\alpha,n)^{21}Ne$

The efficiency of this chain is critically dependent on the uncertain $^{18}O(n,\gamma)^{19}O$ cross section. The large neutron capture cross section of $^{19}F(\langle\sigma\rangle=5.4\pm1.1$ mb at 30 keV; Bao & Käppeler 1987) implies that, in the presence of neutrons, production of ^{19}F by $^{18}O(n,\gamma)^{19}O(\beta^-)^{19}F$ is inhibited by $^{19}F(n,\gamma)^{20}F$. According to test calculations, $\langle\sigma_{18}\rangle$ of the order of 1 mb (at 30 keV) is needed in order to achieve the ^{19}F production levels required by the observations.

Even though the neutron capture cross section at astrophysical energies is likely dominated by a p-wave subthreshold resonance, such a requirement is difficult to reconcile with the measured values of σ_{18} at laboratory thermal energies and at a neutron energy of 200 keV (160 and 15 μb, respectively; McLane et al. 1988). A final evaluation of the merits of this path for ^{19}F synthesis would greatly benefit from a direct measurement of the $^{18}O(n,\gamma)^{19}O$ Maxwellian-averaged cross section at 30 keV.

3.4.5. $^{14}N(\alpha,\gamma)^{18}F(n,\alpha)^{15}N(\alpha,\gamma)^{19}F$ with $^{13}C(\alpha,n)^{16}O$

The main problem with this scenario is that it requires rather high neutron densities ($N_n\geq10^{11}$ cm^{-3}). Although the $^{18}F(n,\alpha)^{15}N$ cross section is not accurately known, it is likely to be large ($\langle\sigma\rangle\approx10^2$–$10^3$ mb at 30 keV), since a resonant level in the compound ^{19}F nucleus lies only 64.3 keV above the $^{18}F+n$ threshold (Ajzenberg-Selove 1987). Given the rather short lifetime of ^{18}F against β decay ($\tau(\beta)=9.5\,10^3$ s), neutron densities $N_n\geq10^{11}$ cm^{-3} are nevertheless required for $^{18}F(n,\alpha)^{15}N$ to dominate $^{18}F(\beta^+)^{18}O$.

The observable diagnostics of the neutron density in AGB stars (i.e. the Rb/Sr ratio or the $^{94}Zr/^{96}Zr$ isotopic ratio) point instead toward N_n in the range 10^8–10^9 cm^{-3} (Lambert 1991). These low values would appear to rule out the present path as responsible for the ^{19}F production in AGB stars. Several comments are in order, however. First of all, this discrepancy between the observed neutron density diagnostics and the neutron density required by $^{14}N(\alpha,\gamma)^{18}F(n,\alpha)^{15}N(\alpha,\gamma)^{19}F$ is relevant only in the case that ^{19}F synthesis and heavy-element synthesis occur during the same neutron burst. The discussion of Sect. 3.3 in connection with Fig. 12 suggested that this may perhaps be the case for the most F-rich stars, but that it is unlikely for the bulk of the S stars with $[F/O]\leq0.5$. Synthesis of ^{19}F is possible with a ^{13}C supply $X_p(^{19}F)\sim X(^{13}C)\lesssim10^{-3}$ (see Fig. 9). But such a limited ^{13}C supply (as well as the presence of the strong neutron poison ^{18}F) then makes heavy-element synthesis inefficient (see Sect. 3.4), so that ^{19}F synthesis cannot be associated with heavy-element synthesis. Since the observed diagnostics characterize the neutron density during the heavy-element synthesis, they are irrelevant to the unrelated ^{19}F synthesis event, during which the neutron density might possibly be higher. When $^{13}C(\alpha,n)^{16}O$ is the neutron source, the neutron density is controlled by the growth rate of the thermal pulse, as ^{13}C from the H-burning ashes is progressively ingested by the growing convective shell (e.g. Hollowell & Iben 1990). The highest mean neutron densities that may be expected in this situation are of the order of 10^9 neutrons cm^{-3}.

In conclusion, the neutron density reached within thermal pulses where $^{13}C(\alpha,n)^{16}O$ is operating appears to be too small to trigger ^{19}F synthesis through the $^{14}N(\alpha,\gamma)^{18}F(n,\alpha)^{15}N(\alpha,\gamma)^{19}F$ path.

3.4.6. Summary

Table 5 summarizes the leaks and constraints of the various paths producing ^{19}F considered in Sects. 3.4.1–3.4.5.

The path that seems most likely to account for the ^{19}F overabundance observed in AGB stars is $^{14}N(\alpha,\gamma)^{18}F(\beta^+)$ $^{18}O(p,\alpha)^{15}N(\alpha,\gamma)^{19}F$ where neutrons and protons come from $^{13}C(\alpha,n)^{16}O$ and $^{14}N(n,p)^{14}C$ (Paper I). This path operates throughout AGB evolution with an efficiency dependent on the initial ^{18}O content of the thermal pulse. In low-temperature pulses with a high ^{18}O initial content, the $^{15}N(p,\alpha)^{12}C$ leak is ineffective so that optimum efficiency gives $^{19}F\sim{}^{13}C(0)$ if $^{13}C(0)\ll{}^{14}N(0)$. However, the dredged-up matter will not only be F-rich, but also ^{18}O-rich, so that the surface $^{16}O/^{18}O$ ratio is predicted to decrease as the F overabundance increases. This correlation is not observed. In higher-temperature pulses where ^{18}O is destroyed by $^{18}O(\alpha,\gamma)^{22}Ne$, ^{19}F synthesis is less efficient due to the $^{15}N(p,\alpha)^{12}C$ leak, but an alteration of the surface $^{16}O/^{18}O$ ratio is no longer predicted. In these situations, the ^{13}C supply from the CNO ashes is insufficient to lead to ^{19}F production at the level $X_p(^{19}F)\sim10^{-4}$–10^{-3} required by the observations. A primary ^{13}C (and concomitant ^{14}N) production has to be invoked to explain the largest F overabundances observed in S and N stars. This requirement is consistent with the fact that the most F-rich stars (for a given $^{12}C/^{16}O$ ratio) show a "CNO excess" resulting from a contamination of their envelope with primary N. We note, however, that a primary production of ^{14}N of the kind studied by Hollowell & Iben (1989, 1990) is unable to increase the F synthesis efficiency. This is because primary ^{13}C and ^{14}N production is restricted in their models to a very thin layer of mass $\sim10^{-4}M_\odot$ that is ultimately ingested by the convective shell of mass $\sim10^{-2}M_\odot$. Although $X(^{13}C)\sim0.02$ and $X(^{14}N)\sim0.04$ in that thin layer, the large dilution factor results in most neutrons being captured by ^{56}Fe, not by ^{14}N, so that the larger neutron supply provided by $^{13}C(\alpha,n)^{16}O$ leads to heavy-element synthesis and not to ^{19}F production. For comparison, $X(^{13}C)\sim10^{-4}$ and $X(^{14}N)\sim0.02$ in the H-burning ashes, but

Table 5. Nuclear paths relevant to ^{19}F synthesis in He-burning environments

Path	$^{14}N(n,\gamma)^{15}N(\alpha,\gamma)^{19}F$
Leaks	$^{14}N(n,^{14}C)p(^{15}N,\alpha)^{12}C$, $^{19}F(n,\gamma)^{20}F$
Constraints	never efficient
Relevance for AGB stars	none
Path	$^{14}N(\alpha,\gamma)^{18}F(n,\alpha)^{15}N(\alpha,\gamma)^{19}F$ with $^{13}C(\alpha,n)^{16}O$
Leaks	$^{18}F(\beta^+)^{18}O$, $^{18}F(n,^{18}O)p(^{15}N,\alpha)^{12}C$
Constraints	$N_n \gtrsim 10^{11}$ cm^{-3}
Relevance for AGB stars	None, because $N_n \lesssim 10^{10}$ cm^{-3} is predicted either from the convective shell growth rate or from the observed N_n diagnostics (Rb/Sr and $^{96}Zr/^{94}Zr$ ratios).
Path	$^{14}N(\alpha,\gamma)^{18}F(\beta^+)^{18}O(p,\alpha)^{15}N(\alpha,\gamma)^{19}F$ with $^{13}C(\alpha,n)^{16}O$ and $^{14}N(n,p)^{14}C$
Leaks	$^{56}Fe(n,\gamma)$, $^{15}N(p,\alpha)^{12}C$
Constraints	$\sigma_{^{14}Nnp}{}^{14}N \gg \sigma_{56}{}^{56}Fe$
Relevance for AGB stars	OK, primary ^{13}C (^{14}N) required for the most F-rich stars.
Path	$^{14}N(\alpha,\gamma)^{18}F(\beta^+)^{18}O(p,\alpha)^{15}N(\alpha,\gamma)^{19}F$ and $^{14}N(\alpha,\gamma)^{18}F(n,\alpha)^{15}N(\alpha,\gamma)^{19}F$ with $^{18}O(\alpha,n)^{21}Ne$ and $^{18}F(n,p)^{18}O$
Leaks	$^{19}F(\alpha,p)^{22}Ne$, $^{18}O(\alpha,\gamma)^{22}Ne$, ($^{15}N(p,\alpha)^{12}C$)
Constraints	high T (i.e. $^{14}N(\alpha,\gamma)^{18}F$ faster than $^{18}F(\beta^+)^{18}O$)
Relevance for the AGB stars	OK, if short exposure to high T and for S stars: primary ^{14}N production (N excess is observed); for N stars: small envelope mass
Path	$^{14}N(\alpha,\gamma)^{18}F(\beta^+)^{18}O(n,\gamma)^{19}O(\beta^-)^{19}F$ with $^{13}C(\alpha,n)^{16}O$ or $^{18}O(\alpha,n)^{21}Ne$
Leaks	$^{19}F(n,\gamma)^{20}F$
Constraints	$\sigma_{^{18}n,\gamma}$ of a few mb, large initial ^{18}O content
Relevance for AGB stars	?

these extend over *half* of the mass of the pulse by which they are engulfed.

Another possible way of producing ^{19}F within thermal pulses involves the same $^{14}N(\alpha,\gamma)^{18}F(\beta^+)^{18}O(p,\alpha)^{15}N(\alpha,\gamma)^{19}F$ chain, but with neutrons and protons coming instead from $^{18}O(\alpha,n)^{21}Ne$ and $^{18}F(n,p)^{18}O$. This scenario requires high-temperature pulses ($T_8 \gtrsim 3$, so that $^{14}N(\alpha,\gamma)^{18}F$ is faster than $^{18}F(\beta^+)^{18}O$), but this requirement might be incompatible with the survival of ^{19}F against $^{19}F(\alpha,p)^{22}Ne$. Several possible ways to circumvent that problem were suggested, however. These include the uncertainties of the current $^{19}F(\alpha,p)^{22}Ne$ reaction rate, a low envelope mass for evolved AGB stars, a very short exposure time to these high temperatures by the dredged-up matter, and a larger ^{19}F production from primary ^{14}N allowing for a limited destructive operation of $^{19}F(\alpha,p)^{22}Ne$.

The $^{14}N(n,\gamma)^{15}N(\alpha,\gamma)^{19}F$ chain is necessarily killed by the $^{15}N(p,\alpha)^{12}C$ poisoning. The $^{14}N(\alpha,\gamma)^{18}F(\beta^+)^{18}O(n,\gamma)^{19}O(\beta^-)^{19}F$ chain is hampered by the low (though uncertain) $^{18}O(n,\gamma)^{19}O$ cross section and the high $^{19}F(n,\gamma)^{20}F$ cross section, along with the branching $^{18}O(p,\alpha)^{15}N$ that will necessarily result from (n, p) reactions on ^{14}N or ^{18}F.

We also noted that the $^{14}N(\alpha,\gamma)^{18}F(n,\alpha)^{15}N(\alpha,\gamma)^{19}F$ chain (with neutrons provided by $^{13}C(\alpha,n)^{16}O$) could have been a good candidate should the convective shell growth rate not have limited the neutron density to $N_n \lesssim 10^9$ cm^{-3}. The high neutron densities required are not in contradiction with observed neutron density diagnostics (Rb/Sr and $^{96}Zr/^{94}Zr$) yielding $N_n \lesssim 10^{10}$ cm^{-3}, in the case that heavy-element and F synthesis are independent events.

The reactions $^{14}N(\alpha,\gamma)^{18}F$, $^{15}N(\alpha,\gamma)^{19}F$, $^{18}F(n,\alpha)^{15}N$, $^{18}F(n,p)^{18}O$, $^{18}O(n,\gamma)^{19}O$, $^{19}F(\alpha,p)^{22}Ne$ are, or may possibly be, important for ^{19}F synthesis in AGB stars. Their cross sections currently suffer from (sometimes quite large) uncertainties. Dedicated nuclear physics studies to reduce these uncertainties would be quite welcome.

4. The galactic origin of ^{19}F

In this section, we address the question of the galactic origin of ^{19}F: can AGB stars account for ^{19}F production at a galactic level, or does the galactic ^{19}F supply originate instead from the ν-process operating in type II supernova, as claimed by Woosley & Haxton (1988) and Woosley et al. (1990), or do both types of objects contribute to galactic ^{19}F?

Answers to this question may be gleaned from both the observed behavior of ^{19}F with metallicity and from the yields provided by each process. As far as the behavior with metallicity is concerned, if ^{19}F comes primarily from SN II events, it may behave as a *primary* element (see Woosley et al. 1990) with respect to ^{16}O, which is also believed to originate from SN II explosions, that is $[^{19}F/H]=[^{16}O/H]$ or $[^{19}F/^{16}O]=0$ in unevolved disk stars. On the other hand, the ^{19}F production in AGB stars is either of primary or secondary origin, depending on the origin of the ^{13}C and ^{14}N seeds (either CNO ashes or primary HHe-b production).

A primary ^{13}C and ^{14}N supply from HHe-b leads to a more efficient ^{19}F production, and may thus be more relevant to

galactic evolution of the F abundance. However, our observations lend some support to the primary production of ^{19}F only in the case of the most F-rich S stars (because of their strong N excess; see Fig. 13), while there is no such evidence in the case of N stars. At the end of Sect. 3.4.3, possible ways for accommodating the large F overabundances of N stars without invoking a primary F production were suggested. It was noted that the largest F overabundances are found among N stars with $^{12}C/^{16}O \lesssim 1.1$, so that the processed matter must have been very F-rich, but only mildly C-rich. The possibility of low-mass envelopes was also invoked.

In summary, it is possible that both primary and secondary F syntheses are found among AGB stars. This is unfortunate, since the two competing sites[5] for ^{19}F production, namely AGB stars and SN II stars, cannot simply be distinguished from the primary or secondary nature of the F synthesis process. Nevertheless, a primary production occurring in AGB stars might still bear a different signature from the one occurring in SN II stars, due to the very different evolutionary timescales of the two types of stars. This is reflected by the different behavior of ^{16}O (mainly coming from massive stars) and ^{56}Fe (mainly produced in SN I stars, originating from intermediate-mass stars), as observed in unevolved disk stars (Wheeler et al. 1989), where $[O/Fe] \sim -0.5\,[Fe/H]$. In other words, if F mainly comes from SN II, $[F/O] \simeq 0$ is expected in *unevolved* disk stars, whereas $[F/Fe] \simeq 0$ or $[F/C] \simeq 0$ expected if F mainly results from primary production in AGB stars.

The case of secondary production in AGB stars is less clear, since $[F/Fe] = [Fe/H]$ is predicted by simple galactic evolution models (under the instantaneous cycling assumption, which is not very good for these long-lived, low-mass AGB stars, however), but a similar prediction for s-process elements is not confirmed by the observations and is a long-standing puzzle in the field of chemical evolution (e.g. Tinsley 1980).

A preliminary check on the behavior of fluorine with metallicity can be attempted from the observation of α Boo (K2 III; $[Fe/H] = -0.56$) yielding $[F/O] = -0.53$, $[F/\bar{M}] = +0.02$. These results are in disagreement with the hypothesis that ^{19}F primarily comes from SN II, and support instead the production by AGB stars. We note, however, that this result is based entirely upon a single, very weak HF line, and the derived abundance is very uncertain.

The amount of ^{19}F injected into the interstellar medium by AGB stars must be large enough to account for the galactic production. A comprehensive discussion would require the use of detailed chemical evolution models, which is beyond the scope of this paper. Despite the inadequacy of the instantaneous recycling approximation, it provides nevertheless useful analytical expressions relating the abundances in unevolved disk stars (or in the primordial solar system) to the nucleosynthetic yields. It is possible to show that, independently of any particular form adopted for the stellar birth rate, the initial mass function or the infall rate (see e.g. Yokoi et al. 1983; Güsten & Mezger 1982), the mass fraction Y_i of species i in the interstellar gas that will be incorporated in new-born stars is proportional to the *net* nucleosynthetic yield $y_i^{\rm net}$, where

$$y_i^{\rm net} = \frac{1}{1-R}\int_{M_0}^{M_{\rm max}} \Delta Q_i(M)\phi(M)\,{\rm d}M,$$

and

$$R = \int_{M_0}^{M_{\rm max}} Q_{\rm ej}(M)\phi(M)\,{\rm d}M$$

is the mass returned to the gas by the dying stars.

In the above expressions, M_0 is the mass of a star whose lifetime equals the age of the galactic disk, $\phi(M)$ is the normalized IMF such that

$$\int_{M_{\rm min}=0.1}^{M_{\rm max}} M\,\phi(M)\,{\rm d}M = 1,$$

$Q_{\rm ej}(M)$ is the mass ejected by a star of initial mass M (i.e. M minus the remnant mass), and $\Delta Q_i(M)$ is the net difference between the mass of element i in the ejecta (freshly produced by nucleosynthesis from another species, as well as initial supply surviving the various nucleosynthesis episodes of the star, the latter being usually referred to as the astrated component) and that in the corresponding material at birth. We note that in the case of a secondary production, $\Delta Q_i(M)$ will itself be a function of the mass fraction Y_j of the seed nucleus j (in the framework of the instantaneous recycling). The ratio of the *net* yields (including astration) of two primary species should then be equal to the ratio of the corresponding abundances in the interstellar gas or, equivalently, in the solar system material (at birth). In the case of F production in AGB stars, carbon provides the best choice as a reference element, since our observations reveal that the production of C and F appears to be well correlated in AGB stars (Fig. 6), and AGB stars are believed to provide most of the galactic carbon supply (Renzini & Voli 1981; Güsten & Mezger 1982; Wheeler et al. 1989). Therefore, the observed F/C ratio in AGB stars should provide a good estimate of the ratio of the corresponding *net* yields due to low- and possibly intermediate-mass stars. From Fig. 6, we find $0.15 \lesssim [F/C]^{\rm S}_{\odot} \lesssim 0.8$ for S stars and $0.2 \lesssim [F/C]^{\rm N}_{\odot} \lesssim 1.12$ for N stars, indicating that the relative yield of F with respect to C is somewhat too large in comparison with the solar system F/C ratio. But massive stars provide a further contribution to the galactic C production (see Güsten & Mezger 1982), and this contribution of C from Type II supernovae can offset the apparently high F/C ratio of the S and N stars.

In any case, since the long timescales involved with low-mass stars might modify the simple predictions derived in the instantaneous recycling framework, numerical models are needed to investigate this question, but this is beyond the scope of the present paper.

The previous discussion, by emphasizing that the F overproduction factor (3 to 30 with respect to the solar system in the most extreme S and N stars) is larger than that of C (2 to 3), suggests that the AGB stars are likely to be major contributors to galactic F production. The claim by Woosley & Haxton (1988) and Woosley et al. (1990) that SN II are instead responsible for the galactic F production is based on similar arguments. For SN II production of F, ^{20}Ne is a suitable reference element, since it is also believed to originate mainly from massive stars. Since Woosley et al. (1990) show that the ^{19}F production is primary in nature, $Y(^{19}F)/Y(^{20}Ne)$ should be equal to $y^{\rm net}_{^{19}F}/y^{\rm net}_{^{20}Ne}$. They found $[^{19}F/^{20}Ne]^{\rm SN\,II}_{\odot} \sim 0$, but this does not take into account the astration of ^{19}F and ^{20}Ne. Here again a more detailed study of the chemical evolution would be desirable.

[5] It should be mentioned that Woosley (1986) suggested that novae could also be a potential site for ^{19}F production.

5. Conclusions

Our observations of F in red giants provide insights into the nucleosynthesis occurring in asymptotic giant branch stars as well as into the much debated question of the stellar site responsible for ^{19}F production at a galactic level. The observed correlation between the [F/O] overabundance and the $^{12}C/^{16}O$ ratio indicates that F can be produced in He-burning environments, confirming the early suggestion by Goriely et al. (1989) from parameterized nucleosynthesis calculations. The $^{14}N(\alpha,\gamma)^{18}F(\beta^+)^{18}O(p,\alpha)^{15}N(\alpha,\gamma)^{19}F$ chain operating at the very beginning of the He-burning with protons provided by $^{14}N(n,p)^{14}C$ and with $^{13}C(\alpha,n)^{16}O$ as a neutron source is most likely responsible for the observed F overabundances in AGB stars. The efficiency of ^{19}F production through this chain is limited by the number of available protons, which is in turn fixed by the initial ^{13}C supply. Under the assumption that $X(^{12}C)=0.2$ in the matter polluting the envelope during the third dredge-up, our observations require $X(^{19}F)\sim 1$ to $2\,10^{-4}$ in that matter in order to account for most of the S stars and $X(^{19}F)$ up to 10^{-3} for the most F-rich S and N stars. In the context of thermal pulses, the ^{13}C supply provided by the CNO ashes left behind the H-burning shell is equal to $X(^{13}C)\sim 10^{-4}$, which can account for the bulk of the S stars. A larger "primary" ^{13}C supply appears necessary for the most F-rich S and N stars. Mixing of protons into the He- and C-rich layer (HHe-burning) must then be invoked. Resolution of the questions raised by our discussion of F overabundances in AGB stars seems certain to lead to greater understanding of the thermal pulses occurring in the He-burning shells of these evolved stars.

Acknowledgements. This work was supported in part by the Robert A. Welch Foundation (Houston) and the National Science Foundation (AST89-02835). A.J. acknowledges a travel grant from IAU Commission 38. J.P. Thibauld kindly provided us with a detailed discussion of the $^{19}F(\alpha,p)^{22}Ne$ reaction rate. Our understanding of ^{19}F nucleosynthesis greatly benefited from discussions with S. Goriely and M. Arnould. We thank K. Hinkle for his expertise with the FTS and in obtaining data from the FTS archives.

References

Ake T.B., 1979, ApJ 234, 471
Anders E., Ebihara M., 1982, Geochim. Cosmochim. Acta 46, 2363
Anders E., Grevesse N., 1989, Geochim. Cosmochim. Acta 53, 197
Ajzenberg-Selove F., 1987, Nucl. Phys. A 475, 1
Aller L.H., 1978, in: Terzian Y. (ed.) Proc. IAU Symp. 76, Planetary Nebulae – Observations and Theory. Reidel, Dordrecht, p. 225
Aller L.H., Czyzak S.J., 1983, ApJS 52, 211
Arnould M., 1991, in: Michaud G., Tutukov A. (eds.) Proc. IAU Symp. 145, Evolution of Stars: The Photospheric Abundance Connection. Kluwer, Dordrecht, p. 287
Bao Z.Y., Käppeler F., 1987, At. Data Nucl. Data Tables 36, 411
Becker S.A., 1981, ApJS 45, 475
Bell R.A., Eriksson K., Gustafsson B., Nordlund Å., 1976, A&AS 23, 37
Boothroyd A.I., Sackmann I.J., 1988, ApJ 328, 653
Brehm K., Becker HW., Rolfs C., Trautvetter H.P., Käppeler F., Ratynski W., 1988, Z. Phys. A330, 167
Brown J.A., Smith V.V., Lambert D.L., Dutchover E. Jr., Hinkle K.H., Johnson H.R., 1990, AJ 99, 1930
Caughlan G.R., Fowler W.A., 1988, At. Data Nucl. Data Tables 40, 283 (CF88)
Cernicharo J., Guélin M., 1987, A&A 183, L10
Dearborn D.S.P., Eggleton P.P., Schramm D.N., 1976, ApJ 203, 455
Denn G.R., Luck R.E., Lambert D.L., 1991, ApJ 377, 657
Despain K.H., Scalo J.M., 1977, ApJ 208, 789
Dominy J.F., 1985, PASP 97, 1104
Dominy J.F., Wallerstein G., Suntzeff N.B., 1986, ApJ 300, 325
Drotleff H.W., Denker A., Hammer J.W., Knee H., Küchler S., Streit D., Rolfs C., Trautvetter H.P., 1991, Z. Phys. A 338, 367
Forestini M., Goriely S., Jorissen A., Arnould M., 1992, A&A 261, 157 (Paper I)
Fowler W.A., Caughlan G.R., Zimmerman B.A., 1967, ARA&A 5, 525
Frantsman Yu.L., 1989, SvA 33, 565
Fujimoto M.Y., 1977, PASJ 29, 331
Goriely S., Jorissen A., Arnould M., 1989, in: Hillebrandt W., Müller E. (eds.) Proc. 5th Workshop on Nuclear Astrophys. (Max Planck Inst. für Astrophys. Rep.), p. 60
Güsten R., Mezger P.G., 1982, Vistas in Astron. 26, 159
Hall D.N.B., Noyes R.W., 1969, Astrophys. Lett. 4, 143
Hall D.N.B., Ridgway S.T., Bell R., Yarborough J.M., 1978, Proc. Soc. Photo-Opt. Instrum. Eng. 172, 121
Herbst W., Racine R., Richer H.B., 1978, PASP 89, 663
Hoffleit D.N., 1982, Bright Star Catalogue (4th ed.) Yale University Obs., New Haven
Hollowell D., Iben I. Jr., 1988, ApJ 333, L25
Hollowell D., Iben I. Jr., 1989, ApJ 340, 966
Hollowell D., Iben I. Jr., 1990, ApJ 349, 208
Iben I. Jr., 1975, ApJ 196, 525
Iben I. Jr., 1976, ApJ 208, 165
Iben I. Jr., 1982, ApJ 280, 821
Iben I. Jr., Renzini A., 1982a, ApJ 259, L79
Iben I. Jr., Renzini A., 1982b, ApJ 263, L23
Iben I. Jr., Renzini A., 1983, ARA&A 21, 271
Iben I. Jr., Kaler J.B., Truran J.W., Renzini A., 1983, ApJ 264, 605
Jaschek C., Conde H., de Sierra A.C., 1964, Catalogue of Stellar Spectra Classified in the Morgan–Keenan System. La Plata Obs., La Plata
Johnson H.R., 1982, ApJ 260, 254
Johnson H.R., Bernat A.P., Krupp B.M., 1980, ApJS 42, 501
Jorissen A., Arnould M., 1989, A&A 221, 161
Keenan P.C., 1954, ApJ 120, 484
Keenan P.C., Boeshaar P.C., 1980, ApJS 43, 379
Koehler P.E., O'Brien H.A., 1989, Phys. Rev. C 39, 1655
Kuperus J., 1965, Physica 31, 1603
Lambert D.L., 1987, JA&A 8, 103
Lambert D.L., 1991, in: Michaud G., Tutukov A. (eds.) Proc. IAU Symp. 145, Evolution of Stars: The Photospheric Abundance Connection. Kluwer, Dordrecht, p. 299
Lambert D.L., Ries L.M., 1981, ApJ 248, 228
Lambert D.L., Gustafsson B., Eriksson K., Hinkle K.H., 1986, ApJS 62, 373

Landré V., Prantzos N., Aguer P., Bogaert G., Lefebvre A., Thibaud J.P., 1990, A&A 240, 85
Lattanzio J.C., 1989, ApJ 344, L25
Lattanzio J.C., 1989, in: Johnson H.R., Zuckerman B. (eds.) IAU Coll. 106, Evolution of Peculiar Red Giant Stars. Cambridge Univ. Press, Cambridge, p. 161
Lattanzio J.C., Malaney R.A., 1989, ApJ 347, 989
McLane V., Dunford Ch.L., Rose Ph.F., 1988, Neutron Cross Sections, Vol. 2. Academic Press, Boston, MA
Nørgaard H., 1980, ApJ 236, 895
Renzini A., Voli M., 1981, A&A 94, 175
Sackmann I.-J., 1980, ApJ 241, L37
Sackmann I.-J., Smith R.L., Despain K.H., 1974, ApJ 187, 555
Scalo J.M., Miller G.E., 1979, ApJ 233, 596
Scalo J.M., Ulrich R.K., 1973, ApJ 183, 151
Scalo J.M., Despain K.H., Ulrich R.H., 1975, ApJ 196, 805
Schönberner D., 1979, A&A 79, 108
Smith V.V., 1984, A&A 132, 326
Smith V.V., 1990, in: Waddington C.J. (ed.) AIP Conf. Proc. 183, Cosmic Abundances of Matter. p. 200
Smith V.V., Lambert D.L., 1985, ApJ 294, 326
Smith V.V., Lambert D.L., 1986, ApJ 311, 843
Smith V.V., Lambert D.L., 1990, ApJS 72, 387
Sneden C., 1974, Ph.D. Thesis, University of Texas at Austin
Spinrad H., Kaplan L.D., Connes P., Connes J., Kunde V.G., Maillard J.P., 1971, in: Lockwood G.W., Dyck H.M. (eds.) Proc. Conf. on Late-type Stars. Contr. Kitt Peak National Observ. 554, 59
Stephenson C.B., 1984, Publ. Warner & Swansey Observ. 3, 1
Thielemann F.-K., Arnould M., 1979, in: Proc. XXII Coll. Liège, Les Elements et leurs Isotopes Dans l'Univers. Liège, Editions de l'Université, p. 59
Tinsley B.M., 1980, Fund. Cosmic Phys. 5, 287
Tipping R.H., 1989, private communication
Utsumi K., 1985, in: Jaschek M., Keenan C. (eds.) Cool Stars with Excesses of Heavy Elements. Reidel, Dordrecht, p. 243
Wallerstein G., 1984, J. Opt. Soc. Am. B 1, 307
Wallerstein G., Torres-Peimbert S., 1968, ApJ 146, 724
Webb D.U., Rao K.N., 1968, J. Mol. Spectrosc. 28, 121
Wheeler J.C., Sneden C., Truran J.W., 1989, ARA&A 27, 279
Wolke K., Härms V., Becker H.W., Hammer J.W., Kratz K.L., Rolfs C., Schröder U., Trautvetter H.P., Wiescher M., Wöhr A., 1989, Z. Phys. A334, 491
Woosley S.E., 1986, in: Audouze J., Chiosi C., Woosley S.E. (eds.) 16th Saas-Fee course, Nucleosynthesis and Chemical Evolution. Geneva Observ., p. 1
Woosley S.E., Haxton W.C., 1988, Nat. 334, 45
Woosley S.E., Fowler W.A., Holmes J.A., Zimmerman B.A., 1978, At. Data Nucl. Data Tables 22, 371
Woosley S.E., Hartmann D.H., Hoffman R.D., Haxton W.C., 1990, ApJ 356, 272
Yamashita Y., 1967, Publ. Dominion Astrophys. Observ. 13, 47
Yamashita Y., 1972, Ann. Tokyo Astron. Observ. 13, 169
Yokoi K., Takahashi K., Arnould M., 1983, A&A 117, 65